SIAM J. NUMER. ANAL.
Vol. 56, No. 5, pp. 3040–3070

A CONSERVATIVE DISCONTINUOUS GALERKIN SOLVER FOR THE SPACE HOMOGENEOUS BOLTZMANN EQUATION FOR BINARY INTERACTIONS*

CHENGLONG ZHANG† AND IRENE M. GAMBA†‡

Abstract. In the present work, we propose a deterministic numerical solver for the space homogeneous Boltzmann equation based on discontinuous Galerkin (DG) methods. Such an application has been rarely studied. The main goal of this manuscript is to generate a conservative solver for the collisional operator. As the key part, the weak form of the collision operator is approximated within subspaces of piecewise polynomials. In order to save the computational cost and to resolve loss of conservation laws due to numerical approximations, we propose the following combined procedures. First, the collision operator is projected onto a subspace of basis polynomials up to first order. Then, at every time step, a *conservation routine* is employed to enforce the preservation of desired moments (mass, momentum, and/or energy) by solving a constrained minimization problem with only linear complexity. The asymptotic error analysis shows the validity and guarantees the accuracy of these two procedures. The approximated collision integral is finally written as a quadratic form in a linear algebra setting. The theoretical number of operations for evaluating the complete set of the approximated *collision matrix* would be of order $O(N^3)$ with N being the total number of freedom for d-dimensional velocity space. However, we have found and applied a "shifting symmetries" property in the collision weight matrix that consists of finding a minimal set of basis matrices that can exactly reconstruct the complete family of such a matrix. This procedure reduces the computation and storage of the collision matrix down to $O(N^2)$. In addition, the matrix is highly sparse, yielding actual complexity $O(N^{2-1/d})$, with d being number of dimensions. Due to the locality of the DG schemes, the whole computing process is well performed with parallelization using hybrid OpenMP and message passing interface. The current work only considers the homogeneous Boltzmann equation with integrable angular cross sections under elastic and/or inelastic interaction laws. No transport is included in this manuscript. We only focus on the approximation of time dynamics for conservative binary collisions. The numerical results on two-dimensional and three-dimensional problems are provided.

Key words. Boltzmann equation, discontinuous Galerkin method, conservative method, parallel computing

AMS subject classifications. 65M60, 65Y05, 45K05, 82B40

DOI. 10.1137/16M1104792

1. Introduction.

The Boltzmann transport equation (BTE) has been the keystone of kinetic theories. Extensive efforts have been put onto the numerical treatments for the nonlinear BTE. The main challenges include, but are not limited to, the high dimensionality of the collision integrals, conservation properties, variable collision mechanism, and so on. The BTE is an integro-differential transport equation, with the solution a phase probability density distribution $f(\mathbf{x}, \mathbf{v}, t)$ measuring the likelihood to find molecules at a location $\mathbf{x}$ with molecular velocities $\mathbf{v}$ at a given time t. The classical BTE models interactions or collisions through a bilinear collision operator, where the collisional kernel models the intramolecular potentials and angular

*Received by the editors November 23, 2016; accepted for publication (in revised form) July 18, 2018; published electronically October 16, 2018.
http://www.siam.org/journals/sinum/56-5/M110479.html
Funding: The work of the authors was partially supported by NSF grants DMS-1413064, DMS-1217154, NSF-RNMS 1107465 and the Moncreif Foundation.
†The Institute for Computational Engineering and Sciences (ICES), University of Texas at Austin, Austin, TX 78712 (chenglongzhng@gmail.com).
‡Department of Mathematics, University of Texas at Austin, Austin, TX 78712 (gamba@math.utexas.edu).

scattering mechanisms known as the angular cross section. These intramolecular potentials model from hard spheres to soft potentials up to Coulombic interactions (important for plasma collisional modeling). The scattering angular function models the anisotropic nature of the interactions. The angular cross sections could be integrable (Grad cutoff kernels) or nonintegrable (Grad noncutoff kernels).

The existence of solutions has been a great mathematical challenge and still remains elusive. Solving the BTE and studying the evolution properties are among the most fundamental problems in fluid dynamics. The numerical approximation to solutions has always been a very challenging problem. Extensive efforts have been put into the numerical treatment of the BTE and other kinetic equations. The main challenges include, but are not limited to, the high dimensionality in the collision operator and revealing the collision mechanism through suitable formulating.

Basically, there are a few classes of computational methods for solving the BTE. One of them is the well-known *direct simulation Monte Carlo* (DSMC) method, which was developed initially by Bird [5] and Nanbu [40] and more recently by [44, 45]. DSMC was developed to calculate statistical moments under near stationary regimes but is not efficient enough to capture transients as well as details of the solution $f(\mathbf{x}, \mathbf{v}, t)$. In addition these methods inherit statistical fluctuations that become a bottleneck in the presence of nonstationary flows or close to continuum regimes. During the last decade, deterministic methods, such as discrete velocity or spectral methods, have been attracting more attention. Discrete velocity models were developed by Broadwell [12] and mathematically studied by Cabannes, Illner, and Kawashima among many authors [13, 36, 37]. More recently these models have been studied for many other applications on kinetic elastic theory in [7, 15, 39, 55, 33, 48, 49, 50]. Spectral methods, which have been originally developed by Gabetta, Pareschi, and Toscani [25] and later by Bobylev and Rjasanow [9] and Pareschi and Russo [43], are supported by the ground breaking work of Bobylev [6] using the Fourier transformed Boltzmann equation to analyze its solutions in the case of Maxwell-type interactions.

More recent implementations of spectral methods for the nonlinear Boltzmann equation are due to Bobylev and Rjasanow [10], who developed a method using the fast Fourier transform (FFT) for Maxwell-type interactions, and then for hard sphere interactions [11] using generalized Radon and X-ray transforms via FFT. Simultaneously, Pareschi and Perthame [42] developed a similar scheme using FFT for Maxwell-type interactions. Later, Ibragimov and Rjasanow [35] developed a numerical method to solve the space homogeneous Boltzmann equation on a uniform grid for variable hard potential interactions with elastic collisions. We mention that, most recently, Filbet and Russo [23, 24] implemented a method to solve the space inhomogeneous Boltzmann equation using the previously developed spectral methods in [43, 42]. Recently, a conservative Lagrangian–Spectral method, which uses Fourier transform as the main tool, was introduced by Gamba and Tharkabhushanam [29, 30], and more recently by Gamba and Haack [31, 32]. It has the capability of approximating solutions to elastic and inelastic collisional models for both isotropic and anisotropic noncutoff angular cross sections. Such spectral scheme is also extended to Landau transport equations modeling collisional plasma in [52], which also combined discontinuous Galerkin (DG) scheme to treat the Vlasov subproblem through operator splitting. For other deterministic schemes, we suggest referring to [4].

While the behavior of the spectral methods may rely on the smoothness of the underlying solutions, in order to capture more irregular features, the DG [21] method may be more appropriate due to its locality and flexibility. It is a finite element method using discontinuous piecewise polynomials as basis functions and numerical fluxes based on upwinding for stability. Please refer to [21] for more details. For problems of

charge transport in semiconductor devices, DG methods are very promising and have provided accurate results at a comparable computational cost [16, 17, 18, 19, 20]. It seems that DG could be a potential method for kinetic equations. However, there are barely any previous work on full nonlinear BTE. To our best knowledge, one attempt might be [34], which deals only with a one-dimensional prototype of BTE. Most recently, Majorana [38] published a work on a DG-based BTE solver. He derived a set of partial differential equations on t, x by a partial application of the DG method, which is only on variable v. The collision invariants are used as a basis to guarantee the conservations laws. However, it is unclear how the collisional integrals are evaluated, and this evaluation actually requires $O(N^3)$ operations. Also very few and limited numerical results were provided. Another more recent work comes from Alekseenko and Josyula [1]. Our scheme was developed independently almost at the same time (see [51]) and is different than the one in [1] in terms of constructing basis functions, evaluating angular cross section integrals, and the enforcing of conservation routines. In addition, we are able to provide asymptotic error analysis. We would like to provide any potential for handling more irregular features in the future, such as rough boundary conditions, etc.

This paper is organized as follows. Section 2 provides some preliminaries about the Boltzmann equations; section 3 explains how to project the collision integrals under our DG scheme and is one of the most important parts, i.e., evaluation of the collision integrals. Some properties are applied to reduce its complexity, which will be explained in section 4. Then, section 5 and section 7 introduce our conservation routine which will be invoked during every time step to enforce preservations of desired moments. Before showing the numerical results in section 8, we provide the asymptotic error analysis in section 6 which verifies that our DG scheme, combined with the conservation routine, provides good approximations to the original Boltzmann problem.

2. The Boltzmann equations. The BTE is an integro-differential transport equation with the solution a phase probability density distribution $f(\mathbf{x}, \mathbf{v}, t) \in \Omega_{\mathbf{x}} \times \mathbb{R}^{d_{\mathbf{v}}} \times \mathbb{R}^+$ (where $\Omega_{\mathbf{x}} \subseteq \mathbb{R}^{d_{\mathbf{x}}}$) measuring the likelihood of finding molecules at a location $\mathbf{x}$ with molecular velocities $\mathbf{v}$ at a given time t. The classical BTE models interactions or collisions through a bilinear collision operator, where the collisional kernel models the intramolecular potentials and angular scattering mechanisms known as the angular cross section. These intramolecular potentials model from hard spheres to soft potentials up to Coulombic interactions (important for plasma collisional modeling). The scattering angular function models the anisotropic nature of the interactions. The angular cross sections could be integrable (Grad cutoff kernels) or nonintegrable (Grad noncutoff kernels).

The BTE with initial boundary values reads

$$\begin{aligned} \frac{\partial f}{\partial t} + \mathbf{v} \cdot \nabla_x f + F(\mathbf{x}, t) \cdot \nabla_v f &= Q(f, f), \\ f(\mathbf{x}, \mathbf{v}, 0) &= f_0(\mathbf{x}, \mathbf{v}), \\ f(\mathbf{x}, \mathbf{v}, t) &= f_B(\mathbf{x}, \mathbf{v}, t), \quad \mathbf{x} \in \partial\Omega_{\mathbf{x}}, \end{aligned} \tag{2.1}$$

where $f = f(\mathbf{x}, \mathbf{v}, t)$. The bilinear integral collisional operator on the right-hand side of (2.1) can be defined weakly or strongly. It encodes the mixing nature of velocity pairs interchange. The strong form goes

$$Q(f, f) = \int_{\mathbf{v}_* \in \mathbb{R}^d, \sigma \in \mathbb{S}^{d-1}} [f' f'_* - f f_*] \, B(|\mathbf{v} - \mathbf{v}_*|, \sigma) \, d\sigma d\mathbf{v}_*, \tag{2.2}$$

where, here and in the following, denote $f' = f(\mathbf{v}')$, $f'_* = f(\mathbf{v}'_*)$ and $f_* = f(\mathbf{v}_*)$ and drop the dependencies on $\mathbf{x}$, t. $\mathbf{v}'$, $\mathbf{v}'_*$ are precollisional velocities corresponding to postcollisional velocities $\mathbf{v}$, $\mathbf{v}_*$. The integration can also parametrized in terms of the center of mass and relative velocity. And on the $d-1$ dimensional sphere, integration is done w.r.t. the unit direction given by the elastic postcollisional relative velocity. The elastic interaction law is reversible; hence pre and postcollisional velocities are interchangeable, obeying

$$\mathbf{u} = \mathbf{v} - \mathbf{v}_*, \quad \mathbf{v}' = \mathbf{v} + \frac{1}{2}(|\mathbf{u}|\sigma - \mathbf{u}), \quad \mathbf{v}'_* = \mathbf{v}_* - \frac{1}{2}(|\mathbf{u}|\sigma - \mathbf{u}). \tag{2.3}$$

Here is the key for the model; the *collision kernel* is modeled by the transition probability rates given by

$$B(|\mathbf{u}|, \sigma) = |\mathbf{u}|^\gamma b(\cos(\theta)), \qquad \gamma \in (-d, 1] \tag{2.4}$$

with *angular cross sections*

$$\cos(\theta) = \frac{\mathbf{u}\cdot\sigma}{|\mathbf{u}|}, \quad b(\cos(\theta)) \sim \sin^{-(d-1)-\alpha}\left(\frac{\theta}{2}\right) \text{ as } \theta \sim 0, \quad \alpha \in (-\infty, 2). \tag{2.5}$$

Without loss of generality, we can assume

$$b(\cos(\theta)) = \frac{1}{2^{d-1}\pi}\sin^{-(d-1)-\alpha}\left(\frac{\theta}{2}\right). \tag{2.6}$$

The regularity parameters γ and α actually correspond to different types of interactions and different power-law molecular potentials. For interaction potentials obeying spherical repulsive laws

$$\phi(r) = r^{-(s-1)}, \quad s \in [2, +\infty),$$

the collision kernel and angular cross section are explicit for $d = 3$; that is, $\gamma = (s-5)/(s-1)$ and $\alpha = 2/(s-1)$ (see [14]). As a convention, $-d < \gamma < 0$ defines soft potentials, $\gamma = 0$ is the Maxwell molecules type interaction, $0 < \gamma < 1$ describes variable hard potentials and $\gamma = 1$ is the classical hard sphere model. Also, the angular cross sections can be of short range or long range; that is, $b(\cos(\theta))$ can be integrable for $\alpha < 0$ and nonintegrable when $\alpha \geq 0$. When $\alpha = 2$, together with $\gamma = -3$, the BTE models the grazing collisions under Coulomb potentials for which the Boltzmann is not well posed. In this case, the model is given by the Fokker–Planck–Landau equations that can be obtained in the grazing collision limit [31].

The weak form, or Maxwell form, associated to the collisional integral (2.2), performed in velocity space is

$$\begin{aligned}\int_{\mathbb{R}^d} Q(f,f)(\mathbf{v})\phi(\mathbf{v})d\mathbf{v} \\ = \int_{\mathbf{v},\mathbf{v}_*\in\mathbb{R}^{2d}} f(\mathbf{v})f(\mathbf{v}_*)\int_{\sigma\in\mathbb{S}^{d-1}} [\phi(\mathbf{v}') + \phi(\mathbf{v}_*{}') - \phi(\mathbf{v}) - \phi(\mathbf{v}_*)]B(|\mathbf{u}|,\sigma)d\sigma d\mathbf{v}_* d\mathbf{v},\end{aligned} \tag{2.7}$$

where now the positive contribution localizes the test function in postcollisional velocity states, while the negative part does the same in their relative precollisional

ones. It is obtained after performing a few change of variables between the pre and postinteraction velocities.

This formulation can also be written in a *double mixing convolution* structure after a change of variable $\mathbf{u} = \mathbf{v} - \mathbf{v}_*$:

$$\int_{\mathbb{R}^d} Q(f,f)(\mathbf{v})\phi(\mathbf{v})d\mathbf{v} = \int_{\mathbf{v},\mathbf{u}\in\mathbb{R}^{2d}} f(\mathbf{v})f(\mathbf{v}-\mathbf{u})G(\mathbf{v},\mathbf{u})d\mathbf{u}d\mathbf{v} \tag{2.8}$$

with

$$G(\mathbf{v},\mathbf{u}) = \int_{\mathbb{S}^{d-1}} \left[\phi\left(\mathbf{v}+\frac{1}{2}|\mathbf{u}|\sigma\right) + \phi\left(\mathbf{v}-\frac{1}{2}|\mathbf{u}|\sigma\right) - \phi(\mathbf{v}) - \phi(\mathbf{v}-\mathbf{u})\right] B(|\mathbf{u}|,\sigma)d\sigma. \tag{2.9}$$

This weak formulation is a fundamental template not only for analytical properties of the solution to the Boltzmann equation but also for the development of deterministic solvers.

Remark. In the current work, we only consider elastic collisions. Yet the proposed DG scheme has no dependency on the restitution coefficient and therefore can be readily extended to the inelastic case.

In spite of its bilinear and nonlocal form, the operator $Q(f,f)$ enjoys many remarkable properties. Among them, the following are most fundamental [14].

Collision invariants and conservation laws. Observing that the elastic interaction law (2.3) is equivalent to the relations

$$\mathbf{v}' + \mathbf{v}'_* = \mathbf{v} + \mathbf{v}_* \quad \text{and} \quad |\mathbf{v}'|^2 + |\mathbf{v}'_*|^2 = |\mathbf{v}|^2 + |\mathbf{v}_*|^2. \tag{2.10}$$

It is easy to check that the weak formulation

$$\int Q(f,f)\phi(\mathbf{v})d\mathbf{v} = \frac{1}{2}\int ff_*[\phi' + \phi'_* - \phi - \phi_*]B(|\mathbf{v}-\mathbf{v}_*|,\sigma)d\sigma d\mathbf{v}_* d\mathbf{v} \tag{2.11}$$

is identical to zero if

$$\phi' + \phi'_* = \phi + \phi_*. \tag{2.12}$$

In addition, the Boltzmann theorem shows that (2.12) holds if and only if $\phi(\mathbf{v})$ is in the space spanned by $\{\phi(\mathbf{v}) = 1, \mathbf{v}, |\mathbf{v}|^2\}$; the $d+2$ test functions, referred to as *collision invariants*, that imply mass, momentum, and kinetic energy,

$$\int_{\mathbb{R}^d} f(\mathbf{v})d\mathbf{v}, \quad \int_{\mathbb{R}^d} \mathbf{v}f(\mathbf{v})d\mathbf{v}, \quad \int_{\mathbb{R}^d} |\mathbf{v}|^2 f(\mathbf{v})d\mathbf{v}, \tag{2.13}$$

respectively, are conserved quantities for solutions $f(\mathbf{v},t)$ of the space homogeneous Boltzmann equation; i.e., these three quantities will remain constant for such flows.

Entropy dissipation and H theorem. In addition, for any $f(\mathbf{v}) > 0$, if set $\phi(\mathbf{v}) = \log f(\mathbf{v})$, then one can prove the following dissipation of entropy

$$\int_{\mathbb{R}^d} Q(f,f)\log f(\mathbf{v})d\mathbf{v} \le 0. \tag{2.14}$$

This dissipation relation actually implies that the equilibrium state will be given by a *Maxwellian distribution*

$$M(\mathbf{v}) = \frac{\rho}{(2\pi T)^{\frac{d}{2}}}\exp\left(-\frac{|\mathbf{v}-\bar{\mathbf{v}}|^2}{2T}\right), \tag{2.15}$$

where ρ is the macroscopic density, $\bar{v}$ the macroscopic velocity, and T the macroscopic temperature ($= R\vartheta$ where ϑ is the absolute temperature, R is a gas constant).

From now on, we focus on the approximation of the Boltzmann equation describing the flow of a probability density $f = f(\mathbf{v}, t)$. Therefore, in the current work, we focus on the approximation to the initial value problem associated to the space homogeneous problem

$$\frac{\partial}{\partial t} f(\mathbf{v}, t) = Q(f, f)(\mathbf{v}, t), \qquad f(\mathbf{v}, 0) = f_0(\mathbf{v}) \tag{2.16}$$

written in its weak form (2.7).

3. The DG projections and evaluations of the collision integrals. We work in the velocity domain $\mathbf{v} \in \mathbb{R}^d$. The general theory of homogeneous Boltzmann equation shows [8, 28] that if $\Omega_{\mathbf{v}}$ is a sufficiently large velocity domain such that the initial state f_0 enjoys most of its mass and energy inside it, then $\Omega_{\mathbf{v}}$ (or one of comparable size) will also contain most of the mass and energy of the solution f for any given time $t > 0$. For example, if the initial state $f_0 \in L^1_{e^{a|\mathbf{v}|^2}}(\mathbb{R}^d)$, then $f(\mathbf{v}, t) \in L^1_{e^{b|\mathbf{v}|^2}}(\mathbb{R}^d)$ for some positive constant $b \leq a$ [2]. Thus, it is reasonable to assume a compact support for the solution and truncate the whole velocity domain to finite $\Omega_{\mathbf{v}} = [-L, L)^d$.

A regular mesh is applied; that is, we divide each direction into N disjoint elements uniformly, such that $[-L, L] = \bigcup_k I_k$, where interval $I_k = [w_{k-\frac{1}{2}}, w_{k+\frac{1}{2}})$, $w_k = -L + (k + \frac{1}{2})\Delta v$, $\Delta v = \frac{2L}{n}$, $k = 0 \ldots n-1$, and thus there is a Cartesian partitioning $\mathcal{T}_h = \bigcup_k E_k$ with uniform cubic element $E_k = I_{k_1} \otimes I_{k_2} \ldots \otimes I_{k_d}$ and multi-index $k = (k_1, k_2, \ldots, k_d)$.

DG methods assume piecewise basis functions; that is,

$$f(\mathbf{v}, t) = \sum_k \mathbf{u}_k(t) \cdot \Phi(\mathbf{v}) \chi_k(\mathbf{v}) \tag{3.1}$$

with $0 \leq |k| < (n-1)^d$; with $\chi_k(v)$ as the characteristic function over the element E_k; coefficient vector $\mathbf{u}_k = (\mathbf{u}_k^0, \ldots, \mathbf{u}_k^l)$, where $l+1$ is the total number of basis functions locally defined on E_k; and basis vector $\Phi(\mathbf{v}) = (\phi_0(\mathbf{v}), \ldots, \phi_l(\mathbf{v}))$.

We choose basis elements $\Phi(\mathbf{v})$ as local polynomial in $P^p(E_k)$, which is the set of polynomials of total degree up to p on E_k. For the sake of convenience, we select the basis such that $\{\phi_i(\mathbf{v}) : i = 0, \ldots, l\}$ are orthogonal.

For example, when $d = 3$, $p = 1$, local linear basis over element E_k can be set as

$$\left\{1, \frac{\mathbf{v}_1 - w_{k_1}}{\Delta v}, \frac{\mathbf{v}_2 - w_{k_2}}{\Delta v}, \frac{\mathbf{v}_3 - w_{k_3}}{\Delta v}\right\}, \tag{3.2}$$

and consequently, the value of f over element E_k is now approximated by

$$f|_{E_k}(\mathbf{v}) = \mathbf{u}_1 + \mathbf{u}_2 \cdot \frac{\mathbf{v}_1 - w_{k_1}}{\Delta v} + \mathbf{u}_2 \cdot \frac{\mathbf{v}_2 - w_{k_2}}{\Delta v} + \mathbf{u}_3 \cdot \frac{\mathbf{v}_3 - w_{k_3}}{\Delta v}. \tag{3.3}$$

The treatment of binary collision operators for Boltzmann-type equations is always important and challenging. The remaining left-hand side, i.e., the advection part of (2.1), would just follow the standard DG finite element method.

By applying the ith basis function on element E_m, $\phi_i(\mathbf{v})\chi_m(\mathbf{v})$ to (2.7) and operating a change of variables $(\mathbf{v}, \mathbf{u}) \leftarrow (\mathbf{v}, \mathbf{v}_*)$, where $\mathbf{u} = \mathbf{v} - \mathbf{v}_*$ is the relative velocity, we obtain

$$\int_{\mathbf{v}\in E_m} Q(f,f)\phi_i(\mathbf{v})dv = \int_{\mathbf{v}\in E_m,\mathbf{v}_*\in\mathbb{R}^d} f(\mathbf{v})f(\mathbf{v}-\mathbf{u}) \cdot \int_{\sigma\in\mathbb{S}^{d-1}} [\phi_i(\mathbf{v}')\chi_m(\mathbf{v}')-\phi_i(\mathbf{v})\chi_m(\mathbf{v})]|\mathbf{u}|^\gamma b\left(\frac{\mathbf{u}\cdot\sigma}{|\mathbf{u}|}\right)d\sigma d\mathbf{u}d\mathbf{v}$$
$$= \sum_k \sum_{\bar{k}} \mathbf{u}_k^T \mathbf{G}_{m,i}(k,\bar{k})\mathbf{u}_{\bar{k}}, \tag{3.4}$$

where we recall the postcollisional velocity $\mathbf{v}' = \mathbf{v} + \frac{1}{2}(|\mathbf{u}|\sigma - \mathbf{u})$. Here, for fixed $k, \bar{k}, m, i$, the entry $\mathbf{G}_{m,i}(k,\bar{k})$ is actually a $(p+1)^d \times (p+1)^d$ matrix, defined as

$$\mathbf{G}_{m,i}(k,\bar{k}) = \int_{\mathbf{v}\in E_k} \int_{\mathbf{v}-\mathbf{u}\in E_{\bar{k}}} \Phi(\mathbf{v})\otimes\Phi(\mathbf{v}-\mathbf{u})\chi_k(\mathbf{v})\chi_{\bar{k}}(\mathbf{v}-\mathbf{u})|\mathbf{u}|^\gamma \cdot \int_{\mathbb{S}^{d-1}} [\phi_i(\mathbf{v}')\chi_m(\mathbf{v}') - \phi_i(\mathbf{v})\chi_m(\mathbf{v})]b\left(\frac{\mathbf{u}\cdot\sigma}{|\mathbf{u}|}\right)d\sigma d\mathbf{u}d\mathbf{v}. \tag{3.5}$$

The key is to evaluate the block entry $\mathbf{G}_{m,i}(k,\bar{k})$ in (3.5). Due to the convolution formulation, the integrals w.r.t. $\mathbf{v},\mathbf{u}$ can be approximated through *triangular quadratures*. Indeed, along each dimension, if $\mathbf{v}_i \in I_{k_i}$, $\mathbf{v}_* \in I_{\bar{k}_i}$, then $(\mathbf{v}_i, \mathbf{u}_i)$ will form a parallelegram which can be divided into two triangles. See Figure 1.

Evaluating the integrals on the sphere takes most of the effort, because one has to figure out how the Cartesian cubes intersect with the spheres. We first extract the angular integrals in (3.5), denoted by $g_{m,i}(\mathbf{v},\mathbf{u})$, and study this form separately:

$$g_{m,i}(\mathbf{v},\mathbf{u}) = \int_{\mathbb{S}^{d-1}} [\phi_i(\mathbf{v}')\chi_m(\mathbf{v}') - \phi_i(\mathbf{v})\chi_m(\mathbf{v})]b\left(\frac{\mathbf{u}\cdot\sigma}{|\mathbf{u}|}\right)d\sigma. \tag{3.6}$$

Then, for any fixed $\mathbf{v},\mathbf{u}$, the postcollisional velocity v' will be on the surface of a ball centered at $\mathbf{v}-\frac{\mathbf{u}}{2}$ with radius $\frac{|\mathbf{u}|}{2}$.

The angular cross section function $b(\cos\theta)$ may have nonintegrable singularity at $\theta = 0$. However, one can avoid the splitting in gain-loss terms in the square bracket in (3.6), where an expansion of the test function in powers of the vector $\mathbf{v}'-\mathbf{v}$ will cancel the singularity in $b(\cos\theta)$ to obtain an integrable, using the fact that $|\mathbf{v}'-\mathbf{v}| = |\mathbf{u}|\sin\frac{\theta}{2}$. The integrability will depend on the singularity of $b(\cos\theta)$ at $\theta = 0$. Our scheme has taken this issue into account.

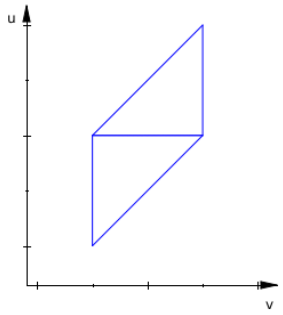

FIG. 1. *Along each dimension,* $(\mathbf{v}_i, \mathbf{u}_i)$ *forms two right triangles.*

The angular integral scheme for evaluating (3.6) proceeds as follows.

1. *Integrable* $b(\cos\theta)$. This case allows to split the "gain" and "loss" terms. Only gain terms involve postcollisional velocity $\mathbf{v}'$ and can be studied separately.

   For $d = 2$, the angular integrals (3.6) can be evaluated analytically. Indeed, for fixed $\mathbf{v}, \mathbf{u}$, the regions over the cycle such that $\mathbf{v}' = \mathbf{v} - 0.5(|\mathbf{u}|\sigma - \mathbf{u}) \in E_m$ can be exactly performed by solving a system of trigonometric relations by setting $\sigma = (\sin\gamma, \cos\gamma) \in S^1(\mathbb{R}^2)$ and finding

$$\begin{cases} \mathbf{v}_1 + 0.5(|\mathbf{u}|\sin\gamma - \mathbf{u}_1) \in I_{m_1}, \\ \mathbf{v}_2 + 0.5(|\mathbf{u}|\cos\gamma - \mathbf{u}_2) \in I_{m_2}. \end{cases} \tag{3.7}$$

   We have built a programmable routine of deriving all possible overlapped intervals of γ.

   Similarly, for the case $d = 3$, setting $\sigma = (\sin\gamma\cos\varphi, \sin\gamma\sin\varphi, \cos\gamma) \in S^2(\mathbb{R}^3)$, we solve the corresponding trigonometric relations

$$\begin{cases} \mathbf{v}_1 + 0.5(|\mathbf{u}|\sin\gamma\cos\varphi - \mathbf{u}_1) \in I_{m_1}, \\ \mathbf{v}_2 + 0.5(|\mathbf{u}|\sin\gamma\sin\varphi - \mathbf{u}_2) \in I_{m_2}, \\ \mathbf{v}_3 + 0.5(|\mathbf{u}|\cos\gamma - \mathbf{u}_3) \in I_{m_3}. \end{cases} \tag{3.8}$$

   The third inequality will give a range for the polar angle γ w.r.t. a preferred direction, and all integrals w.r.t γ will be performed by adaptive quadratures, say, CQUAD in the GNU Scientific Library (GSL) [27]. In particular, for any fixed γ, the first two relations will decide the range of azimuthal angle φ exactly (by invoking the routine mentioned above).

   We stress that angle γ above is not necessarily the scattering angle θ defined in (2.5).

2. *Nonintegrable* $b(\cos\theta)$. In this case, we need a more delicate strategy approach based on an specific choice of angle parametrization that enables a cancellation of the angular singularity. While we include this strategy for completeness of the scheme description, the numerical implementation of this approach will be performed in future work on for the computation of the spectral gap of the linearized Boltzmann equation for nonintegrable cross section [53].

   Thus, we now consider a local spherical coordinate system with $\mathbf{u}$ being the polar direction, i.e., $\cos\theta = \frac{\mathbf{u}\cdot\sigma}{|\mathbf{u}|}$, as defined in ((2.5)). We show that our scheme builds a programmable routine of deriving all possible overlapped intervals of θ by taking a transformation that rotates the polar direction back onto z-axis of the Cartesian coordinate system.

   Such orthogonal rotation matrix A can be constructed explicitly for the following two cases.

   Case $d = 2$:

$$A = \frac{1}{|\mathbf{u}|}\begin{pmatrix} -\mathbf{u}_2 & \mathbf{u}_1 \\ \mathbf{u}_1 & \mathbf{u}_2 \end{pmatrix}. \tag{3.9}$$

   Then, $z = \frac{|\mathbf{u}|}{2}A^T\left(\sin\theta, \cos\theta - 1\right)^T$ and $\sigma = A^T\left(\sin\theta, \cos\theta\right)^T$,

Case $d = 3$:

$$A = \frac{1}{|\mathbf{u}|}\begin{pmatrix} \frac{\mathbf{u}_1\mathbf{u}_3}{\sqrt{\mathbf{u}_1^2+\mathbf{u}_2^2}} & \frac{\mathbf{u}_2\mathbf{u}_3}{\sqrt{\mathbf{u}_1^2+\mathbf{u}_2^2}} & -\sqrt{\mathbf{u}_1^2+\mathbf{u}_2^2} \\ -\frac{\mathbf{u}_2|\mathbf{u}|}{\sqrt{\mathbf{u}_1^2+\mathbf{u}_2^2}} & \frac{\mathbf{u}_1|\mathbf{u}|}{\sqrt{\mathbf{u}_1^2+\mathbf{u}_2^2}} & 0 \\ \mathbf{u}_1 & \mathbf{u}_2 & \mathbf{u}_3 \end{pmatrix}, \tag{3.10}$$

where we assume $\mathbf{u}_1^2 + \mathbf{u}_2^2 \neq 0$, otherwise; the rotation matrix is reduced to the identity matrix.

In the three-dimensional case, we set $\mathbf{z} = \frac{|\mathbf{u}|}{2}A^T(\sin\theta\cos\varphi, \sin\theta\sin\varphi, \cos\theta - 1)^T$, $\sigma = A^T(\sin\theta\cos\varphi, \sin\theta\sin\varphi, \cos\theta)^T$.

With this framework, changing the unitary $\sigma \leftarrow A^{-1}\sigma = A^T\sigma$ and recalling postcollisional velocity $\mathbf{v}' = \mathbf{v} + \frac{1}{2}(|\mathbf{u}|\sigma - \mathbf{u})$ yields the angular integration (3.6) in the convolutional form

$$\begin{aligned} g_{m,i}(\mathbf{v},\mathbf{u}) &= \int_{\mathbb{S}^{d-1}} \left[\phi_i \circ \chi_m(\mathbf{v}+\mathbf{z}) - \phi_i \circ \chi_m(\mathbf{v})\right] b(\cos\theta)\, d\sigma \\ &= \int_{\mathbb{S}^{d-1}} \left[\phi_i \circ \chi_m\left(\mathbf{v} - \frac{\mathbf{u}}{2} + \frac{|\mathbf{u}|}{2}\sigma\right) - \phi_i \circ \chi_m(\mathbf{v})\right] b(\cos\theta)\, d\sigma. \end{aligned}$$

We take $d = 3$ for example. The whole domain of (θ, φ), i.e., the sphere, can be divided into the following four subdomains:

(1) $S_1 = [0, \theta_0] \times [0, 2\pi]$;
(2) $S_2 = [\theta_0, \theta_1] \times I_\varphi(\theta)$;
(3) $S_3 = [\theta_0, \theta_1] \times ([0, 2\pi] \setminus I_\varphi(\theta))$; and
(4) $S_4 = [\theta_1, \pi] \times [0, 2\pi]$,

where the angles θ_0, θ_1 and intervals $I_\varphi(\theta)$ are determined according to the following strategy: When $\mathbf{v} \in E_m$, $\sin\frac{\theta_0}{2} = \min(1, \frac{1}{|\mathbf{u}|}\mathrm{dist}(\mathbf{v}, \partial E_m))$ since $|\mathbf{z}| = |\mathbf{u}|\sin\frac{\theta}{2}$; when $\mathbf{v} \notin E_m$, θ_0 is the smallest possible θ such that $\mathbf{v}'$ lies in E_m. The angle θ_1 is the largest possible θ such that $\mathbf{v}'$ lies in E_m. The sets $I_\varphi(\theta)$ are intervals for φ, depending on θ, such that $\mathbf{v}'$ lies in E_m.

Due to the characteristic functions in the integrands of $g_{m,i}(\mathbf{v},\mathbf{u})$ (3.11), we have the following four cases:

(a) 0-0: the case when $\mathbf{v}' \notin E_m$ and $\mathbf{v} \notin E_m$ is trivial since it contributes nothing to the final weight matrix.
(b) 1-0: the case when $\mathbf{v}' \in E_m$ but $\mathbf{v} \notin E_m$, the effective domain (where $g_{m,i}(\mathbf{v},\mathbf{u}) \neq 0$) is $(\theta, \varphi) \in S_2$, and

$$g_{m,i}(\mathbf{v},\mathbf{u}) = \int_{S_2} \phi_i(\mathbf{v}')b(\cos\theta)\sin\theta\, d\theta d\varphi.$$

(c) 0-1: the case when $\mathbf{v}' \notin E_m$ but $\mathbf{v} \in E_m$, the effective domain is $(\theta, \varphi) \in S_3 \cup S_4$, and

$$g_{m,i}(\mathbf{v},\mathbf{u}) = -\int_{S_3 \cup S_4} \phi_i(\mathbf{v})b(\cos\theta)\sin\theta\, d\theta d\varphi.$$

(d) 1-1: the case when $\mathbf{v}' \in E_m$ and $\mathbf{v} \in E_m$, the effective domain is $(\theta, \varphi) \in S_1 \cup S_2$, and

$$g_{m,i}(\mathbf{v},\mathbf{u}) = \int_{S_1 \cup S_2} \left[\phi_i(\mathbf{v}') - \phi_i(\mathbf{v})\right] b(\cos\theta)\sin\theta\, d\varphi d\theta.$$

Here we need to pay special attention to the integration over S_1, where the singularity cancelled. Recall $\phi_i(\mathbf{v})$ are polynomial basis locally defined on each element E_m and $\mathbf{v}' = \mathbf{v} + \mathbf{z}$. Since $\mathbf{z} \sim \mathbf{0}$, we take the Taylor expansion of $\phi_i(\mathbf{v}')$ around $\mathbf{v}$,

$$\phi_i(\mathbf{v}') - \phi_i(\mathbf{v}) = \nabla\phi_i(\mathbf{v}) \cdot \mathbf{z} + \frac{1}{2}\mathbf{z}^T\nabla^2\phi_i(\mathbf{v})\mathbf{z} + O(|\mathbf{z}|^3).$$

So, it is not hard to observe that, for terms with lowest power of $\sin\theta$, the azimuthal angle φ will be integrated out and leave only powers of $1 - \cos\theta$, which will help cancel the singularity in $b(\cos\theta)$ from (2.6). That is,

$$\begin{aligned}
&\int_0^{\theta_0}\int_0^{2\pi} [\phi_i(\mathbf{v}') - \phi_i(\mathbf{v})]\, b(\cos\theta)\sin\theta d\varphi d\theta \\
&\qquad \le C\int_0^{\theta_0} (1-\cos\theta)\sin^{-2-\alpha}\frac{\theta}{2}\sin\theta d\varphi d\theta \\
&\qquad \le C\int_0^{t_0} t^{1-\alpha} dt \\
&\qquad = \frac{C}{2-\alpha} t_0^{2-\alpha}
\end{aligned}$$

after performing the change of integration coordinates $t = \sin\frac{\theta}{2}$ for $t_0 = \sin\frac{\theta_0}{2}$ and noticing that $\alpha < 2$.

In practice, the sets S_1 and S_2 can be combined. The outer integration w.r.t. the polar angle θ is performed using adaptive quadratures, say, CQUAD in GSL [27], and the inner integration w.r.t. φ is done analytically by calling a similar routine that derives all possible intervals of φ.

Remark. The above routine can be only applied to the case when $\mathbf{v}, \mathbf{v}'$ fall onto the same mesh element (when collision is almost grazing); for other cases, the angular cross sections can be regarded as integrable (far away from grazing collisions) and thus can call routines in "integrable $b(\cos\theta)$."

After the angular integration terms $g_{m,i}(\mathbf{v}, \mathbf{u})$ is performed, plugging it back into (3.5), we obtain the block matrix $\mathbf{G}_{m,i}(k, \bar{k})$.

Next, denoting the whole coefficient vector $\mathbf{U} = (\mathbf{u}_0, \ldots, \mathbf{u}_{M-1})^T$ with $\mathbf{u}_k = (\mathbf{u}_k^0, \ldots, \mathbf{u}_k^l)^T$ and $M = ((l+1)n)^d$ the total number of degrees of freedom, then the semi-discrete DG form of the homogeneous Boltzmann equation (2.16) reads

$$\frac{d\mathbf{U}}{dt} = \mathbf{Q}(\mathbf{U}) \tag{3.11}$$

with initial data being the L^2 projection of $f_0 = f(\mathbf{v}, 0)$. Here the collision vector $\mathbf{Q} = (\mathbf{Q}_0, \ldots, \mathbf{Q}_{M-1})^T$, and each block $\mathbf{Q}_m$ is of size $(l+1)^d \times 1$ with its ith component being denoted by $\mathbf{Q}_m^i$,

$$\mathbf{Q}_m^i = \sum_k \sum_{\bar{k}} \mathbf{u}_k^T \mathbf{G}_{m,i}(k, \bar{k}) \mathbf{u}_{\bar{k}}\,. \tag{3.12}$$

Thus, we obtain the componentwise formulation of (3.11)

$$\frac{d\mathbf{u}_m^i}{dt} = \sum_k \sum_{\bar{k}} \mathbf{u}_k^T \mathbf{G}_{m,i}(k, \bar{k}) \mathbf{u}_{\bar{k}}\,. \tag{3.13}$$

We will call the matrix $\mathbf{G}_{m,i}$ the *Boltzmann collision matrix* or simply *weight matrix.*

4. Computing and storage complexity of collision matrix reduction strategy. When computing the approximated weight function $\mathbf{G}_{m,i}(k,\bar{k})$ of size $M\times M$ from (3.5) for every test function $\phi_i(\mathbf{v})$ defined over element E_m, theoretically, the total computing and storage complexity for the weights would be $O(M^3)$, which can be very expensive.

However, the following features of the collision matrices are crucial for reducing the weight complexity. They are

- temporally independent and precomputed,
- shifting symmetries,
- sparse,
- parallelizable.

4.1. Shifting symmetry property for uniform meshes. Here we assume a uniform mesh. First we observe the fact that the postcollisional velocity is calculated using the law $\mathbf{v}' = \frac{\mathbf{v}+\mathbf{v}_*}{2} + \frac{|\mathbf{v}-\mathbf{v}_*|}{2}\sigma$, which performs shifts both in v_* and v fixed. These shifts depend on the spherical integration in a bounded domain, i.e., $\sigma \in E_m$.

Thus, it can be seen that the same shift on both $\mathbf{v} \in E_k$ and $\mathbf{v}_* \in E_{\bar{k}}$ lands the value of $\mathbf{v}'$ for the same shift.

Moreover, considering we work with locally supported basis functions, then the evaluation of (3.5) will remain invariant for as long as the relative positions between E_k ($E_{\bar{k}}$) and test element E_m keep unchanged, and at the same time, the piecewise basis functions $\phi(\mathbf{v})$ on E_m are only valued locally upon the relative position of $\mathbf{v}$ inside E_m.

This property is summarized as follows.

Shifting symmetry property. If the basis piecewise polynomials $\phi(\mathbf{v})$, defined over element E_m, are functions of $\frac{\mathbf{v}-\mathbf{w}_m}{\Delta v}$ (where $\mathbf{w}_m$ is the center of cube E_m), then the family of collision matrix $\{\mathbf{G}_{m,i}\}$ in (3.5) satisfies the shifting symmetry property

$$\mathbf{G}_{m,i}(k,\bar{k}) = \mathbf{G}_{\tilde{m},i}(k-(m-\tilde{m}),\bar{k}-(m-\tilde{m})), \tag{4.1}$$

where $m,\tilde{m},k,\bar{k}$ are d-dimensional multi-indices, and $i = 0,\dots,(l+1)^d$.

Indeed, recall that $\mathbf{G}_{m,i}(k,\bar{k})$ is the block matrix evaluated at $v \in E_k$, $v_* \in E_{\bar{k}}$, and the ith test function over element E_m. Since the basis functions $\phi(\mathbf{v})$ are locally defined on E_m and only valued at $\frac{\mathbf{v}-\mathbf{w}_m}{\Delta v}$, the value of $\phi(\mathbf{v})$ will stay invariant as long as elements E_k and E_m are shifted by the same amount. Without loss of generality, we assume basis functions are piecewise constants. Then the integrals in (3.5) now are

$$\mathbf{G}_m(k,\bar{k}) = \int_{\mathbf{v}\in E_k}\int_{\mathbf{v}_*=\mathbf{v}-\mathbf{u}\in E_{\bar{k}}} |\mathbf{u}|^\gamma \int_{\mathbb{S}^{d-1}} [\chi_m(\mathbf{v}')-\chi_m(\mathbf{v})] b\left(\frac{\mathbf{u}\cdot\sigma}{|\mathbf{u}|}\right) d\sigma d\mathbf{u} d\mathbf{v}. \tag{4.2}$$

Suppose now a different test function over $E_{\tilde{m}}$ is applied, which means the element E_m is shifted to $E_{\tilde{m}}$. Notice the gain-loss terms in the square bracket in (4.2); it's not hard to find that the gain and loss will remain the same as long as $\mathbf{v}$ and $\mathbf{v}'$ stay at the same relative position to the test element. That said, the indices for $\mathbf{v}$ and $\mathbf{v}'$ should be shifted by the same amount $\tilde{m}-m$. This is easily achievable by noticing the elastic collision law: that the indices for precollisional velocities $\mathbf{v}$ and $\mathbf{v}_*$ should be shifted by same amount $\tilde{m}-m$. Meanwhile, the same shift on $\mathbf{v}$ and $\mathbf{v}_*$ leads to invariant relative velocity $\mathbf{u}$. Thus, we obtain another block matrix $\mathbf{G}_{\tilde{m}}(k+\tilde{m}-m,\bar{k}+\tilde{m}-m)$ which is valued the same as $\mathbf{G}_m(k,\bar{k})$.

This shifting procedure can be illustratively shown in Figure 2 for a one-dimensional problem with piecewise constant basis functions.

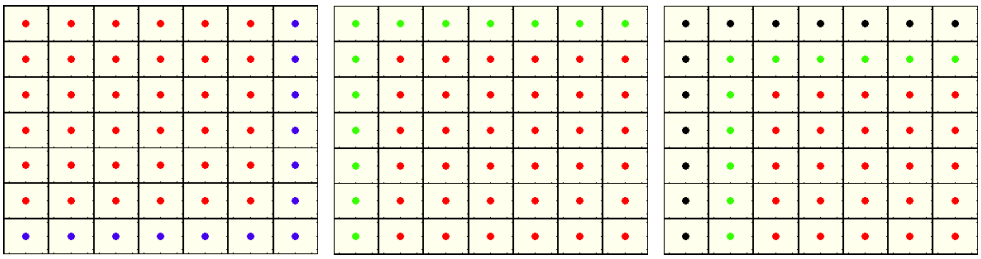

FIG. 2. *Dots (entries) of the same color are shifted to the neighboring matrices.*

This property inspires us to seek possible ways to reduce the actual computing complexity of all the collision matrices.

THEOREM 4.1. *There exists a minimal basis set of matrices*

$$\mathfrak{B} = \{G_{m,i}(k,\bar{k}) : \textit{For } j = 1 \dots d \textit{ if } m_j \neq 0, k_j \times \bar{k}_j = 0; \\ \textit{if } m_j = 0, k_j, \bar{k}_j = 0, 1, \dots, n-1\},$$

which can exactly reconstruct the complete family $\{\mathbf{G}_{m,i}\}$ *through shifting.*

Proof. Indeed, without loss of generality, let us only consider piecewise constant basis functions, i.e., $i = 0$. And we start from only one layer on one dimension or let us imagine a one-dimensional prototype problem, i.e., $G_m(k,\bar{k})$ where $m, k, \bar{k}$ are one-dimensional indices. This is corresponding to one velocity component. The complete family $\{\mathbf{G}_m\}$ will be the tensor product of all layers.

For any $m \neq 0$ $(m = 1, \dots, n-1)$, the entries $G_m(k,\bar{k})$ are obtained through shifting according to the following policy:

$$G_m(k,\bar{k}) = \begin{cases} G_0(k-m, \bar{k}-m) \text{ if } k, \bar{k} \geq m, \\ G_l(0, \bar{k}-k) \text{ with } l = 1 \dots m \text{ if } \bar{k} \geq k,\ k < m, \\ G_l(k-\bar{k}, 0) \text{ with } l = 1 \dots m \text{ if } k \geq \bar{k},\ \bar{k} < m, \end{cases} \tag{4.3}$$

which recover the complete set of entries $G_m(k,\bar{k})$. None of the entries in the basis set is shifting-equivalent. And it is not hard to observe that if one drops any entry in the basis set, it will be impossible to recover the original complete family. Thus, we conclude that the set $\mathfrak{B}$ is one minimal basis set. ∎

As seen from Theorem 4.1, along each dimension, we only need to compute and store the full matrix for $m = 0$, and the first rows and columns for all other m's. This requires a computing and storage complexity bounded by $3n^2$. For d dimensions, the total complexity will be bounded by $3^d N^2$ with $N = n^d$. Hence, in the actual algorithm, we only need to compute the minimal set $\mathfrak{B}$, which requires a computing complexity of only $O(N^2)$.

4.2. Sparsity. The matrices in the set $\mathfrak{B}$ are actually highly sparse. The sparsity of $\mathfrak{B}$, again, comes from $\mathbf{v}' = \mathbf{v} - \frac{\mathbf{u}}{2} + \frac{|\mathbf{u}|}{2}\sigma$. The postcollisional velocity v' is on the sphere parametrized by $\sigma \in S^{d-1}$, centered at $\frac{\mathbf{v}+\mathbf{v}_*}{2}$, and with radius given by $|\mathbf{u}|/2$. Thus, not all binary particle collisions between velocities $\mathbf{v} \in E_k$ and $\mathbf{v}_* \in E_{\bar{k}}$ could

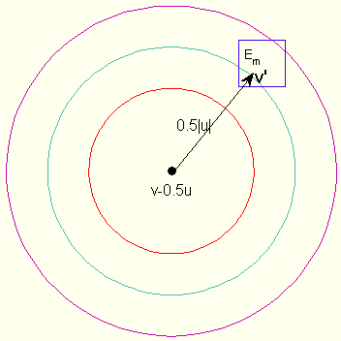

FIG. 3. *Velocities v, u such that v' lies in mesh element E_m.*

TABLE 1
The computing and storage complexity of basis $\mathfrak{B}$.

n	Wall clock time (s)	Order	♯ of nonzeros	Order
8	3.14899	\	812884	\
12	39.3773	6.2301	6826904	5.2484
16	228.197	6.1075	30225476	5.1717
20	893.646	6.1176	94978535	5.1311
24	2686.72	6.0375	241054134	5.1054

collide ending up with a postcollisional velocity $\mathbf{v}'$ lying in a given fixed element E_m. Figure 3 illustrates such conditions.

Since, for each $\mathbf{v}$ and $\mathbf{v}_*$ fixed, the sphere that contains $\mathbf{v}'$ and $\mathbf{v}'_*$ in a binary collision is a $(d-1)$-manifold embedded in d dimensions, the counting of such interactions is nonzero when such sphere intersects with element E_m. This results in only an $O(n^{2d-1})$ of nonzeros in the set $\mathfrak{B}$.

Therefore, while by Theorem 4.1, the calculations of the weights $G_m(k, \bar{k})$ can be made in an algorithm with computational complexity of $O(n^{2d})$, we conjecture that the corresponding storage complexity is of $O(n^{2d-1})$. Indeed, we verify this order complexity with a test run for $d = 3$ in Table 1 done on a single core of Xeon E5-2680 2.7 GHz processor (on cluster Stampede at the Texas Advanced Computing Center, TACC [47]).

4.3. Parallelization. The whole weight matrices are only computed once and stored for further use. Due to the locality of DG schemes, the whole process of computing $\mathfrak{B}$ can be well performed using hybrid message passing interface (MPI, a standardized distributed computing infrastructure) [26] and OpenMP [41]. The collision weight matrices quantify the contributions of the binary collisions to the evolution of the distribution functions. For each grid point on the distribution function, the time evolution is attributed to all possible binary collisions. Furthermore, different grid points do not need to communicate with each other. Thus, one can distribute all grid points across the computing node community while keeping the grid information accessible to each computing node within the community. This is done using MPI. To further parallelize the computing, on each node, the working load computing, for example, of matrix entries and matrix-vector computations is shared among threads, using OpenMP.

Figure 4 shows the parallel efficiency of strong scaling for computing some sets of the basis matrix.

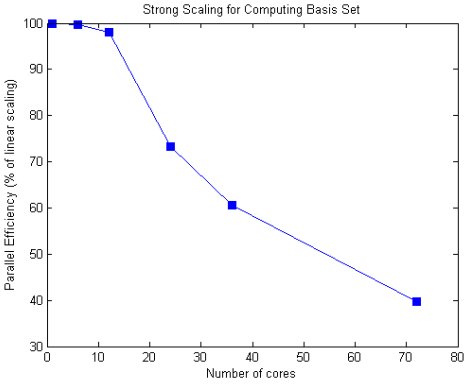

FIG. 4. *The strong scalability of computing collision matrix (n=18).*

5. Conservation routines. The above approximate collision operator Q doesn't preserve the moments as desired due to the truncation of velocity domain. To achieve the conservation properties, following the ideas in [29], we design an intermediate routine to force the conservations. This routine will be implemented as a *L^2-distance minimization problem* with the constraints the preservation of desired moments. The optimization problem can be solved through the *Lagrange multiplier method*.

The conservation of moments for the approximate solution $f_h(t, \mathbf{v})$ goes, for any time t,

$$\int_{\Omega_{\mathbf{v}}} f_h(t,\mathbf{v})\varphi(\mathbf{v})d\mathbf{v} = \int_{\Omega_{\mathbf{v}}} f_{h,0}(\mathbf{v})\varphi(\mathbf{v})d\mathbf{v}, \tag{5.1}$$

where $\varphi(\mathbf{v})$ is one of the $d+2$ collision invariants $1, \mathbf{v}_1, \ldots, \mathbf{v}_d, |\mathbf{v}|^2$.

So, our objective is to solve the following.

Conservation routine (functional level). Minimize in the Banach space

$$\mathcal{B}^e = \left\{ X \in L^2(\Omega_{\mathbf{v}}) : \int_{\Omega_{\mathbf{v}}} X = \int_{\Omega_{\mathbf{v}}} X\mathbf{v} = \int_{\Omega_{\mathbf{v}}} X|\mathbf{v}|^2 = 0 \right\}$$

the functional

$$\mathcal{A}^e(X) := \int_{\Omega_{\mathbf{v}}} \left(Q_{uc}(f)(\mathbf{v}) - X\right)^2 d\mathbf{v}. \tag{5.2}$$

Recalling the DG approximation for $f_h(t, \mathbf{v})$ in (3.1) and the time evolution for $f_h(t, \mathbf{v})$ (3.11), one can get the conservation requirements on the approximation collision vector $\mathbf{Q}$, defined in (3.11),

$$\mathbf{CQ} = \mathbf{0}, \tag{5.3}$$

where the $(d+2) \times M$ dimensional constraint matrix writes

$$\mathbf{C}_{:,j} = \begin{pmatrix} \int_{E_k} \phi_l(\mathbf{v})d\mathbf{v} \\ \int_{E_k} \phi_l(\mathbf{v})\mathbf{v}d\mathbf{v} \\ \int_{E_k} \phi_l(\mathbf{v})|\mathbf{v}|^2 d\mathbf{v} \end{pmatrix} \tag{5.4}$$

with ϕ_l the lth basis function on element E_k and the column index $j = (p+1)k + l = 0, \ldots, M-1$.

To force the conservation, we seek for the L^2-distance closest to $\mathbf{Q}_c$, which is the minimizer of the following constrained optimization problem.

Conservation routine (discrete level). Find $\mathbf{Q}_c$, the minimizer of the problem

$$\begin{aligned} &\min \frac{1}{2}(\mathbf{Q}_c - \mathbf{Q})^T \mathbf{D}(\mathbf{Q}_c - \mathbf{Q}) \\ &\text{such that} \quad \mathbf{C}\mathbf{Q}_c = \mathbf{0}. \end{aligned}$$

Due to the orthogonality of the local basis, $\mathbf{D}$ is a positive definite diagonal matrix with its jth entry $\frac{1}{|E_k|}\int_{E_k}(\phi_l(\mathbf{v}))^2 d\mathbf{v}$, $j = (p+1)k + l$. For example, in three dimensions, when $p = 0$, $\mathbf{D}$ is reduced to an identity matrix; when $p = 1$, with the orthogonal basis chosen in (3.2),

$$\mathbf{D} = \text{Diag}\left(1, \frac{1}{12}, \frac{1}{12}, \frac{1}{12}, 1, \frac{1}{12}, \frac{1}{12}, \frac{1}{12}, 1, \ldots\right).$$

Remark. Note that with spectral method in [29], the corresponding discrete optimization problem actually takes D to be an identity matrix. This is because the L^2 norm is aymptotically preserved by the l^2 norm of its Fourier coefficients.

To solve the minimization problem, we employ the Lagrange multiplier method. Denote by $\lambda \in \mathbb{R}^{d+2}$ the multiplier vector. Then the objective function is

$$\mathcal{L}(\mathbf{Q}_c, \lambda) = \frac{1}{2}(\mathbf{Q}_c - \mathbf{Q})^T \mathbf{D}(\mathbf{Q}_c - \mathbf{Q}) - \lambda^T \mathbf{C}\mathbf{Q}_c. \tag{5.5}$$

Solving by finding the critical value of $\mathcal{L}$ gives

$$\begin{cases} \dfrac{\partial \mathcal{L}}{\partial \mathbf{Q_c}} = \mathbf{0} \\ \dfrac{\partial \mathcal{L}}{\partial \lambda} = \mathbf{0} \end{cases} \Longrightarrow \begin{cases} \mathbf{Q}_c = \mathbf{Q} + \mathbf{D}^{-1}\mathbf{C}^T\lambda \\ \mathbf{C}\mathbf{Q}_c = \mathbf{0} \end{cases} \Longrightarrow \lambda = -(\mathbf{C}\mathbf{D}^{-1}\mathbf{C}^T)^{-1}\mathbf{C}\mathbf{Q}.$$

(Here, notice that $\mathbf{C}\mathbf{D}^{-1}\mathbf{C}^T$ is symmetric and positive definite and hence its inverse exists.)

Thus, we get the minimizer $\mathbf{Q}_c$

$$\mathbf{Q}_c = [\mathbb{I}d - \mathbf{D}^{-1}\mathbf{C}^T(\mathbf{C}\mathbf{D}^{-1}\mathbf{C}^T)^{-1}\mathbf{C}]\mathbf{Q}, \tag{5.6}$$

where $\mathbb{I}d$ is an identity matrix of size $M \times M$. So, $\mathbf{Q}_c$ is a perturbation of $\mathbf{Q}$.

So, the final conservative semidiscrete DG formulation for the homogeneous equation is

$$\frac{d\mathbf{U}}{dt} = \mathbf{Q}_c. \tag{5.7}$$

Obviously it preserves the desired moments. And what's more, we expect the approximate solution approaches a stationary state. This is guaranteed by analyzing the convergence behavior.

6. Asymptotic behavior. The asymptotic error analysis is based on the work [3]. Readers can find more details of the proofs for many theorems and estimates invoked here. Some main results and analysis tools being used in this section are also listed in the appendix.

Since we are working under a DG framework, it might be necessary to summarize some of the notations and properties regarding DG approximations, which are introduced at the beginning of Appendix A.

Now, let us go to the asymptotic error analysis. We assume $f \in C([0,T]; L^2(\mathbb{R}^d))$ to be the solution to the homogeneous BTE (2.16) with initial $f_0 = f(\mathbf{v}, 0)$. The Galerkin method allows us to take the L^2 projection, $P_h : L^2(\Omega_v) \to L^2(\Omega_v)$, on both sides of the BTE (2.16)

$$\frac{\partial}{\partial t} P_h f(\mathbf{v}, t) = P_h Q(f)(\mathbf{v}, t) \text{ in } [0,T] \times \Omega_v. \tag{6.1}$$

We introduce the concept of *extension operator* (Appendix A.1) $E : H^\alpha(\Omega_v) \to L^2(\mathbb{R}^d)$, which will be used in future derivations. Its properties are summerized in [3].

The collision operator $Q(f)$ is global in velocity. It is reasonable to expect $P_h Q(f) \sim P_h Q(E P_h f)$ for accurate enough projectors (or small enough mesh size h). Thus the solution to

$$\frac{\partial}{\partial t} g(\mathbf{v}, t) = P_h Q(Eg)(\mathbf{v}, t) \tag{6.2}$$

will be a good approximation to $P_h f$, the solution to projected (6.1).

This is not enough, because we are limited to the conservation properties. So, actually the following initial value problem is studied in our asymptotic analysis, whose solution is expected to approximate the solution f of the original homogeneous BTE (2.16).

$$\begin{aligned} \frac{\partial}{\partial t} g(\mathbf{v}, t) &= Q_c(g)(\mathbf{v}, t), \\ g_0(\mathbf{v}) &= P_h f(\mathbf{v}, 0), \end{aligned} \tag{6.3}$$

where $Q_c(g)$ is the conservation correction to the following unconserved operator $Q_{uc}(g)$:

$$Q_{uc}(g)(\mathbf{v}, t) = P_h(Q(Eg)\chi_{\Omega_v})(\mathbf{v}, t), \tag{6.4}$$

where χ_{Ω_v} is the characteristic function on the truncated domain Ω_v. It follows that

$$\|Q_{uc}(f_h)\|_{L^2(\Omega_v)} \lesssim \|Q(Ef_h)\|_{L^2(\Omega_v)} \lesssim \|Q(f)\|_{L^2(\Omega_v)}. \tag{6.5}$$

As is shown in the last section, the conservation correction is the minimizer of the L^2-distance to the projected collision operator subject to mass, momentum, and energy conservation. It can be shown that the conserved projection operator $Q_c(f_h)$ is a perturbation of $Q_{uc}(f_h)$ by a second order polynomial. See Theorem 3.3 in [3] for the conservation correction estimate (or see Appendix A.2).

Let us summarize our major estimate result first.

THEOREM 6.1 (H^{p+1}-error estimate). *Fix $k', k \geq 0$, and assume nonnegative initial density function $f_0 \in L^1_2 \cap H^{p+1}_q(\mathbb{R}^d)$ with $q = \max\{k + k', 1 + \frac{d}{2\gamma}\}$, $0 < \gamma \leq 1$ is the defined in collision kernel* (2.4). *g is the DG solution of* (6.3), *where the piecewise basis polynomials are of order at most p. For a given simulation time T and index $\alpha \leq p + 1$, there exists an extension E_{p+1}, a lateral size $L_0(T, f_0)$ for domain Ω_v, and a small grid diameter $h_0(T, L, f_0, \alpha)$ for triangulation $\mathcal{T}_h$ of Ω_v such that for any $L \geq L_0$, $h \leq h_0$,*

$$\sup_{t\in[0,T]}\|f-g\|_{H^\alpha_k(\mathcal{T}_h)}\le C_{k'}e^{C_kT}\left(O(L^{\gamma k+\alpha}h^{p+1-\alpha})+O(L^{-\gamma k'})\right),$$

where $h=max_{E_v\in\mathcal{T}_h}diam(E_v)$ *is the maximal grid diameter for the regular triangulation* $\mathcal{T}_h$ *of* Ω_v*; the constants* C_k *and* $C_{k'}$ *depend on* H^{p+1}_q*-norms and moments of* f_0*.*

Proof. The proofs can be easily extended from the one in [3]. But here to make the work complete, we would like to briefly explain how the proofs go. The readers can refer to [3] for more details.

We will first prove the case $\alpha=0$, i.e., the L^2_k estimate, and then follow an induction on the index α.

One can easily observe that, in domain Ω_v,

$$\frac{\partial}{\partial t}(f-g)=Q(f,f)-Q_c(g)=(Q(f,f)-Q(Eg,Eg))+(Q(Eg,Eg)-Q_c(g)). \tag{6.6}$$

Denote $e_h=\|f-g\|_{L^2_k(\mathcal{T}_h)}$. Multiply on both sides of the above (6.6), piecewise, by $(f-g)\langle v\rangle^{2\gamma k}$ restricted over each element of the triangulation $\mathcal{T}_h$, and sum over all the elements; we get

$$\frac{1}{2}\frac{\partial e_h^2}{\partial t}=I_1+I_2. \tag{6.7}$$

We estimate I_1 and I_2 separately.

$$\begin{aligned}I_1&=\int_{\mathcal{T}_h}\langle v\rangle^{2\gamma k}(f-g)(Q^+(f+Eg,f-Eg)+Q^+(f-Eg,f+Eg))\\&\quad-\int_{\mathcal{T}_h}\langle v\rangle^{2\gamma k}(f-g)(Q^-(f+Eg,f-Eg)-\int_{\mathcal{T}_h}\langle v\rangle^{2\gamma k}(f-g)Q^-(f-Eg,f+Eg))\\&\lesssim\|f-g\|^2_{L^2_k(\mathcal{T}_h)}+\|f-g\|_{L^2_k(\mathcal{T}_h)}\left(\|f\|_{L^2_{k+1/2}(\mathbb{R}^d\setminus\Omega_v)}+\|g\|_{L^2_{k+1/2}(\Omega_v\setminus\delta^{-1}\Omega_v)}\right),\end{aligned}$$

where δ is the dilation parameter of the extension operator; $\lesssim$ means the estimate constants are independent of parameters T,L,h but only information (norms, moments, etc.) of f,g themselves. Here, the uniform propagation of higher order moments of f,g are applied. See Lemma 4.2 in [3].

By Holder's inequality and conservation correction estimate,

$$\begin{aligned}I_2&=\int_{\mathcal{T}_h}\langle v\rangle^{2\gamma k}(f-g)(Q(Eg,Eg)-Q_c(g))\\&\lesssim L^{\gamma k}\|f-g\|_{L^2_k(\mathcal{T}_h)}\left(\|Q(Eg,Eg)-Q_{uc}(g)\|_{L^2(\mathcal{T}_h)}+\delta^{2k'}\mathrm{O}_{d/2+\gamma(k'-1)}\|g\|_{L^1_{k'}(\mathcal{T}_h)}\right),\end{aligned}$$

where and in the following we apply notation $\mathrm{O}_r:=O(L^{-r})$.

So, combining the above estimates for I_1 and I_2 gives us

$$\frac{de_h(t)}{dt}\le Ce_h(t)+\varepsilon(t)+\varpi(t),$$

where, by the standard approximation theory in the broken Sobolev spaces,

$$\begin{aligned}\varepsilon(t)&:=CL^{\gamma k}\|Q(Eg,Eg)-Q_{uc}(g)\|_{L^2(\mathcal{T}_h)}\\&\lesssim L^{\gamma k}h^{p+1}\|Q(Eg,Eg)\|_{H^{p+1}(\Omega_v)}\\&\lesssim L^{\gamma k}h^{p+1}\|g\|^2_{H^{p+1}_\mu(\Omega_v)}\quad\left(\mu>1+\frac{d}{2\gamma}\right)\end{aligned}$$

and

$$\varpi(t) := C\left(\|f\|_{L^2_{k+1/2}(\mathbb{R}^d\setminus\Omega_v)} + \|g\|_{L^2_{k+1/2}(\Omega_v\setminus\delta^{-1}\Omega_v)}\right) + \mathrm{O}_{d/2+k'-k-s}\|Ef_h\|_{L^1_{k'}(\Omega_v)}$$
$$= \delta^{2k'}\mathrm{O}_{\gamma(k'-k-1/2)}\left(\|f\|_{L^2_{k'}(\mathbb{R}^d)} + \|g\|_{L^2_{k'}(\Omega_v)} + \|g\|_{L^1_{k'}(\Omega_v)}\right) \le \mathrm{O}_{\gamma k'}.$$

Gronwall's inequality implies

$$\sup_{t\in[0,T]}\|f-g\|_{L^2_k(\mathcal{T}_h)} \le \left(\|f_0 - f_{h,0}\|_{L^2_k(\mathcal{T}_h)} + \int_0^T \varepsilon(s)ds + \sup_{t\in[0,T]}\varpi(t)\right)e^{CT} \tag{6.8}$$

for any $T>0$. The lateral size $L(T,f_0)$, $h \le h_0(T,L,f_0)$ are decided following the same argument in Theorem 5.1 in [3].

Additionally, by the standard approximation theory,

$$\|f_0 - f_{h,0}\|_{L^2_k(\mathcal{T}_h)} \lesssim L^{\gamma k}h^{p+1}\|f_0\|_{H^{p+1}(\Omega_v)}.$$

Thus, the case $\alpha = 0$ is proved. Assume the result is true for any multi-index $\beta < \alpha \le p+1$. Then similarly following the above procedures,

$$\frac{\partial}{\partial t}\|\partial^\alpha(f-g)\|^2_{L^2_k(\mathcal{T}_h)} \le I_1 + I_2 + I_3.$$

Using the Leibniz formula and the smoothing effect of the positive collision operator,

$$I_1 := \int_{\mathcal{T}_h}\langle v\rangle^{2\gamma k}\partial^\alpha(f-g)\partial^\alpha(Q(f,f)-Q(Eg,Eg))$$
$$\lesssim \|\partial^\alpha(f-g)\|^2_{L^2_k(\mathcal{T}_h)} + \text{ lower order terms.}$$

A typical lower order term is given by

$$\|\partial^\alpha(f-g)\|_{L^2_k(\mathcal{T}_h)}\|\partial^{\alpha-\beta}(f+Eg)\|_{L^2_{k+\mu}(\mathbb{R}^d)}\|\partial^\beta(f-Eg)\|_{L^2_{k+1}(\mathbb{R}^d)}.$$

By induction hypothesis,

$$\|\partial^\beta(f-Eg)\|_{L^2_{k+1}(\mathbb{R}^d)}$$
$$:\le \|\partial^\beta(f-g)\|_{L^2_{k+1}(\mathcal{T}_h)} + \|\partial^\beta f\|_{L^2_{k+1}(\mathbb{R}^d\setminus\Omega_v)} + \|\partial^\beta Eg\|_{L^2_{k+1}(\mathbb{R}^d\setminus\Omega_v)}$$
$$\le C_{k'}e^{C_kT}\left(O(L^{\gamma(k+1)+\beta}h^{p+1-\beta}) + \delta^{2(k+k')}O(L^{-\gamma k'})\right)$$
$$\le C_{k'}e^{C_kT}\left(O(L^{\gamma k+\alpha}h^{p+1-\alpha}) + \delta^{2(k+k')}O(L^{-\gamma k'})\right),$$

where the last inequality holds as long as $h \le L^{1-\gamma}$.

For I_2, by Holder's inequality and the conservation correction estimate,

$$I_2 := \int_{\mathcal{T}_h}\langle v\rangle^{2\gamma k}\partial^\alpha(f-g)\partial^\alpha(Q_c(g)-Q_{uc}(g))$$
$$\le \|\partial^\alpha(f-g)\|_{L^2_k(\mathcal{T}_h)}\|\partial^\alpha(Q_c(g)-Q_{uc}(g))\|_{L^2_k(\mathcal{T}_h)}$$
$$\le \|\partial^\alpha(f-g)\|_{L^2_k(\mathcal{T}_h)}\left(L^{\gamma k}\|Q(Eg,Eg)-Q_{uc}(g)\|_{L^2(\mathcal{T}_h)} + \delta^{2k''}\mathrm{O}_{d/2+\gamma(k''-k)}\right).$$

For I_3, by Holder's inequality and approximation theory,

$$\begin{aligned} I_3 &:= \int_{\mathcal{T}_h} \langle v\rangle^{2\gamma k}\partial^\alpha(f-g)\partial^\alpha(Q_{uc}(g)-Q(Eg,Eg)) \\ &\le L^{\gamma k}\|\partial^\alpha(f-g)\|_{L^2_k(\mathcal{T}_h)}\|\partial^\alpha(Q_{uc}(g)-Q(Eg,Eg))\|_{L^2(\mathcal{T}_h)} \\ &\lesssim L^{\gamma k}\|\partial^\alpha(f-g)\|_{L^2_k(\mathcal{T}_h)}h^{p+1-\alpha}\|g\|^2_{H^{p+1}_{d/2+\gamma}}. \end{aligned}$$

Finally, we get

$$\begin{aligned} &\frac{\partial}{\partial t}\|\partial^\alpha(f-g)\|_{L^2_k(\mathcal{T}_h)} \\ &\quad\le C\|\partial^\alpha(f-g)\|_{L^2_k(\mathcal{T}_h)} + C_{k'}e^{C_kT}\left(O(L^{\gamma k+\alpha}h^{p+1-\alpha}) + \delta^{2(k+k')}O(L^{-\gamma k'})\right); \end{aligned}$$

therefore, Gronwall's inequality will give us the final estimate. ∎

7. Temporal evolution. The approximate solution will be solved at the level of discrete time. That is, $t_{n+1} = t_n + \triangle t$, where $\triangle t$ is the time step size. Since there are no high order derivatives or diffusive natures in the homogeneous Boltzmann equation, no CFL condition is imposed. The only restriction on time step size may be that Δt should be less than the dimensionalized mean free time. So, we can choose the simplest forward *Euler scheme*, which is explicit in time. At each time step, the conservation routine, denoted *CONSERVE*, designed in the last section will be called to force conservations.

So, suppose $\mathbf{U}_n$ is the coefficient vector (thus the solution) computed at the current time t_n; then the solution for the next time step is obtained through the following routines:

$$\begin{aligned} &\mathbf{Q}_n = \text{COMPUTE}(\mathbf{U}_n)\,, \\ &\mathbf{Q}_{c,n} = \text{CONSERVE}(\mathbf{Q}_n)\,, \\ &\mathbf{U}_{n+1} = \mathbf{U}_n + \triangle t\mathbf{Q}_{c,n}\,. \end{aligned}$$

The Euler scheme is formally first order in time. For higher order accuracy, a higher order Runge–Kutta scheme can be used whenever necessary. The conservation routine has to be invoked at every intermediate step of the Runge–Kutta scheme.

At each time step, for the evolution of each mesh element, we have to compute a quadratic form (3.13) which inevitably involves $O(n^9)$ (in $d = 3$) operations in total. However, due to the sparsity, the actual order of number of operations for each time step is $O(n^8)$, which is indeed a large number. Fortunately, the reconstructions of collision matrices and computing of quadratic form (3.13) are well parallelizable for each Euler step. See Table 2 for the results on time for one single temporal step of evolution and Table 3 for results on the parallelization for one step of time evolution. Both tests run on Xeon Intel 3.33 GHz Westmere processors (on cluster Lonestar-TACC [47]).

From Table 2 we can see the time consumed for one single step grows with an order slightly less than 8. This is normal, because during time evolution and reconstruction of the whole collision matrix, we only need to retrieve those effective (nonzero) matrix entries through shifting of the basis set $\mathfrak{B}$ (see Theorem 4.1). The grid points (index m) and associated effective entries (indices $k, \bar{k}$) are shifted together. Thus, in practice, not every grid point requires a full ergodic of the weight matrix, or in other words, many grid points only need a partial access to the weight

TABLE 2
The wall clock time for one temporal evolution step.

n	Wall clock time (s)	Order
16	18.3362	\
18	47.6001	8.0993
20	105.155	7.5227
22	216.818	7.5923
24	419.533	7.5862
26	781.282	7.7683

TABLE 3
The parallelization for one temporal evolution step, for $n = 24$.

Number of cores	Wall clock time (s)
1	459.967
2	341.771
6	181.561
12	144.485
24	129.691
36	107.907
48	90.2676
72	74.2794

matrix. Table 3 actually shows a low strong scaling efficiency (speedup is far from linear). This is not surprising because we need to call a parallelized reconstruction process for each time step, then gather information together and redistribute them to the computing community. And furthermore, we have to call the conservation routine, which is essentially serial, at each time step. In addition, when computing the basis set $\mathfrak{B}$, we choose to distribute grid points across the computing nodes while the basis information associated with each grid point m (see Theorem 4.1) is not of equivalent size; for example, for $m = 0$ the full matrix is computed, while for another m's, only the first row and column are computed. Hence, some processing elements, for example, the one containing $m = 0$, have to be accessed much more frequently than others, also causing an unbalanced distribution of computing resources.

8. Numerical results. Test 1 is a two-dimensional Maxwell type of elastic collisions, benchmarked by *Bobylev–Krook–Wu* exact solutions. The initial density distribution is

$$f(\mathbf{v}, 0) = \frac{|\mathbf{v}|^2}{\pi\delta^2}\exp(-|\mathbf{v}|^2/\delta^2). \tag{8.1}$$

This problem has an exact solution [22]

$$f(\mathbf{v}, t) = \frac{1}{2\pi s^2}\left(2s - 1 + \frac{1-s}{2s}\frac{|\mathbf{v}|^2}{\delta^2}\right)\exp\left(-\frac{|\mathbf{v}|^2}{2s\delta^2}\right), \tag{8.2}$$

where $s = 1 - \frac{1}{2}\exp(-\delta^2 t/8)$. In the test, we choose the scaling parameter $\delta = \pi/6$ such that the truncation domain is well chosen by $\Omega_v = [-\pi, \pi]$. We let it run for 600 time steps with $\Delta t = 0.1$. This example is used to test the accuracy by calculating the relative L^2 errors compared to its exact solution and relative entropy verifying that the numerical solution will converge to the true equilibrium. See Figure 5 for the evolution of the marginal density distributions; Figure 6 and Figure 7 show the relative L^2 errors and relative entropy, respectively. The marginal density distribution is defined as

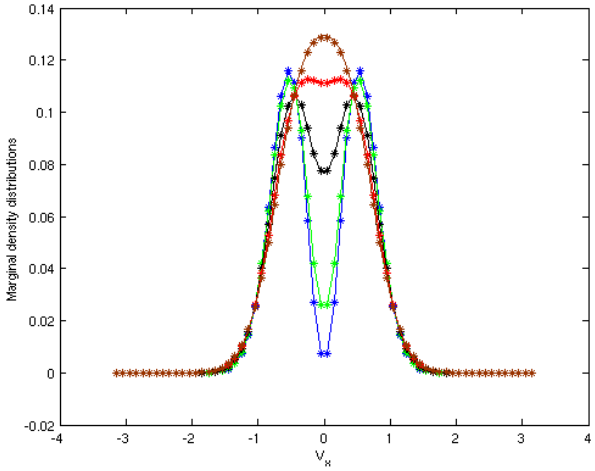

FIG. 5. *Test* 1*: Comparison of solutions at time* $t = 0, 1, 5, 10, 15s$*.* $n = 44$ *per direction; solid line: exact solution, stars: piecewise constant approximation.*

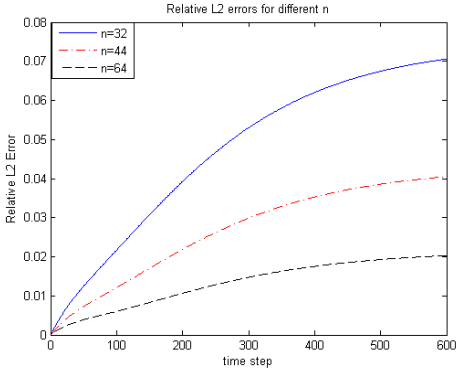

FIG. 6. *Test* 1*: Relative* L^2 *errors, compared with true solution, for different numbers of mesh elements.*

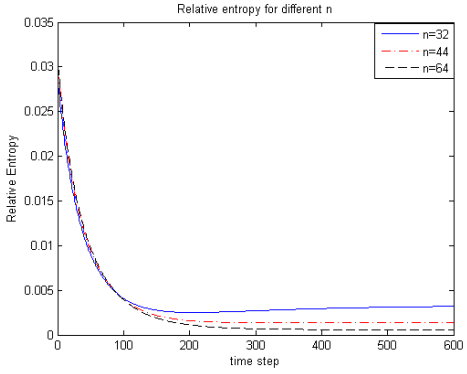

FIG. 7. *Test* 1*: Relative entropy for different numbers of mesh elements.*

$$f_x(\mathbf{v}_x \in I_k) = \frac{1}{(\Delta v)^2} \int_{I_k} \int_{I_{n/2}} f(\mathbf{v}, t) d\mathbf{v}_x d\mathbf{v}_y.$$

The relative L^2 error is defined as

$$\frac{\left(\int_{\Omega_v} |f_h(\mathbf{v}, t) - f(\mathbf{v}, t)|^2 dv\right)^{1/2}}{\left(\int_{\Omega_v} |f(\mathbf{v}, t)|^2 dv\right)^{1/2}}.$$

The relative entropy given by

(8.3)

$$\mathcal{H}_{rel}(t) = \int_{\Omega_v} f(\mathbf{v}, t) \log f(\mathbf{v}, t) - f_M(\mathbf{v}) \log f_M(\mathbf{v}) d\mathbf{v} = \int_{\Omega_v} f(\mathbf{v}, t) \log \frac{f(\mathbf{v}, t)}{f_M(\mathbf{v})} d\mathbf{v},$$

where $f_M(\mathbf{v})$ is the true equilibrium density distribution and is expected to converge to zero which implies the solution converges to the true equilibrium in the sense of L^1.

Remark. In Test 1, numerical simulation results (although not presented here) can show that our scheme propagates positivity for any given positive time, if initially so, for piecewise constant basis functions. Meanwhile, the conservation laws (here, only mass due to the zeroth order of basis polynomials) are expected to hold but only for a short time. The constrained minimization problem that enforces the $d+2$ collision invariants brakes the positivity propagation. We stress that the traditional limiters reconstruction technique, which focuses on the positivity reconstruction of spatial fluxes in the transport operator, can only ensure preservation of mass as shown in Cheng, Gamba, and Proft [20] for a linear Boltzmann collision operator that can only have one conservation law (mass). We note that the positivity preservation technique by Zhang and Shu [54] for higher order basis functions works for scalar conservation laws that only have one conserved quantity (i.e., mass). In fact, enforcing the Gauss–Lobatto quadratures for positivity flux reconstruction on DG schemes for the nonlinear Boltzmann collision operator results in an overdetermined set of equations with no solution.

We stress that the Lagrangian constrained minimization problem presented in section 5, which enforces the preservation of collision invariants, mitigates the effects of negativity, as shown the Alonso, Gamba, and Tharkabhushaman in [3]. It is shown that the numerical solution converges to the equilibrium Maxwellian associated to the initial data, in the case of the space homogeneous Boltzmann problem. This implies that, for large time, the negativity points occur at the tails of the probability distribution function, for which the solution will be close to zero (below machine accuracy) in the properly chosen computational frame. In addition, it is shown in [3], that as long as the "negative energy" (second order moment of the negative part of the density function) stays under control by a small ratio to the "positive energy," the system is not only stable, but also the accuracy of the numerical approximations is guaranteed.

Test 2 is also a two-dimensional Maxwell type of elastic collisions. This example is used to show the conservation routines. The initial states we take are convex combinations of two shifted Maxwellian distributions (see Figure 8).

Truncate the velocity domain $\Omega = [-4.5, 4.5]^2$, and set number of nodes in each velocity direction $n = 32.40$. The initial densitv function is a convex combination of two Maxwellians:

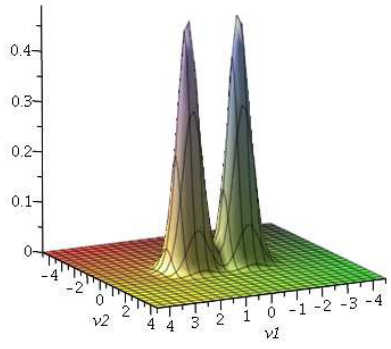

FIG. 8. *Test 2: Initial probability distribution: Two shifted Maxwellians.*

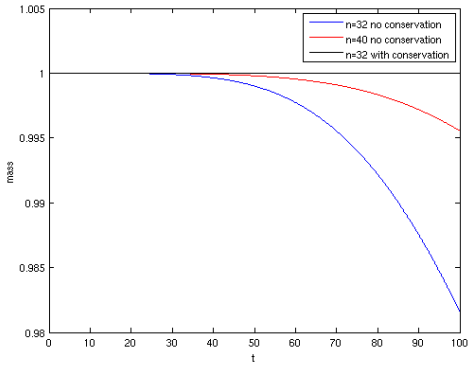

FIG. 9. *Test 2: Evolution of mass.*

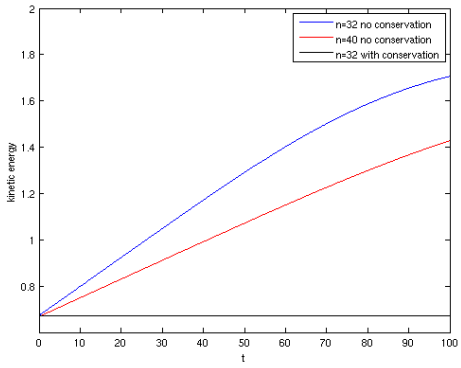

FIG. 10. *Test 2: Evolution of kinetic energy.*

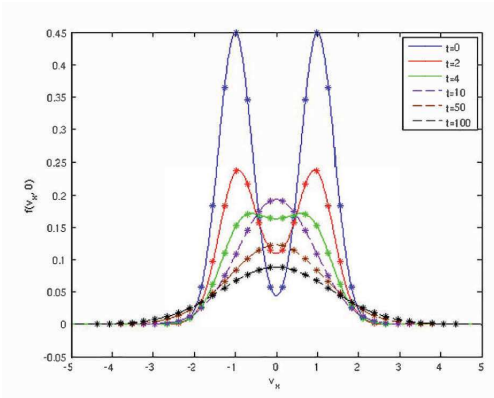

FIG. 11. *Test 2: Evolution of PDF without conservation routines.*

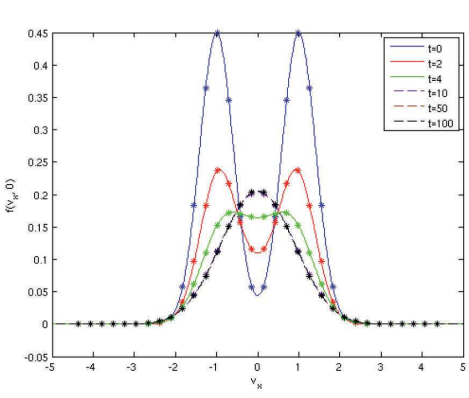

FIG. 12. *Test 2: Evolution of PDF with conservation routines.*

$$f_0(\mathbf{v}) = \lambda M_1(\mathbf{v}) + (1-\lambda) M_2(\mathbf{v}), \tag{8.4}$$

with $M_i(\mathbf{v}) = (2\pi T_i)^{-d/2} e^{-\frac{|\mathbf{v}-\mathbf{V}_i|^2}{2T_i}}$, $T_1 = T_2 = 0.16$, $\mathbf{V}_1 = [-1, 0]$, $\mathbf{V}_2 = [1, 0]$, and $\lambda = 0.5$.

We test for $n = 32$ and $n = 40$ for 1000 time steps to compare the results and see the long time behavior as well. The probability density distribution functions are reconstructed with splines.

From Figure 9 and Figure 10, we can see, the scheme with piecewise constant test functions, as expected, conserves moments for short time; in the long run, due to the truncation, the tails of the density functions are lifted up and thus moments are expected to lose. At the same time, finer grids indeed give more accuracy. Since the basis polynomials are only zero order, it is expected that mass is much better conserved than higher order moments.

Through the comparison of Figure 11 and Figure 12 we see, after long time, with no conservation routine, the density distribution collapses due to the truncation of

the domain. However, with conservation routines, the density function stays stable when reaching equilibrium. So, the conservation routine works and is necessary for stability. However, the cost we pay is the loss of positivity.

Test 3 is initialized by a sudden jump on temperatures, i.e., a jump discontinuity in its initial state and far from equilibrium, as shown in Figure 13. The initial state is given by

$$f_0(\mathbf{v}) = \begin{cases} \dfrac{1}{2\pi T_1} \exp\left(-\dfrac{|\mathbf{v}|^2}{2T_1}\right), & \mathbf{v}_1 \le 0, \\ \dfrac{1}{2\pi T_2} \exp\left(-\dfrac{|\mathbf{v}|^2}{2T_2}\right), & \mathbf{v}_1 > 0, \end{cases}$$

with $T_1 = 0.3$ and $T_2 = 0.6$. The collision is of type two-dimensional hard spheres.

With truncated domain $\Omega_{\mathbf{v}} = [-5, 5]$, $n = 44$ in each direction, the DG solution well captures the discontinuity and converges to equilibrium. See Figure 14 and Figure 15.

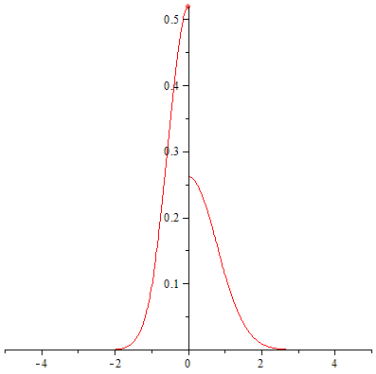

FIG. 13. *Test 3: Initial density function.*

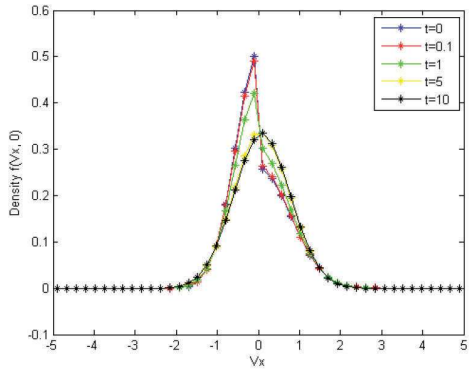

FIG. 14. *Test 3: DG solutions for sudden heating problem.*

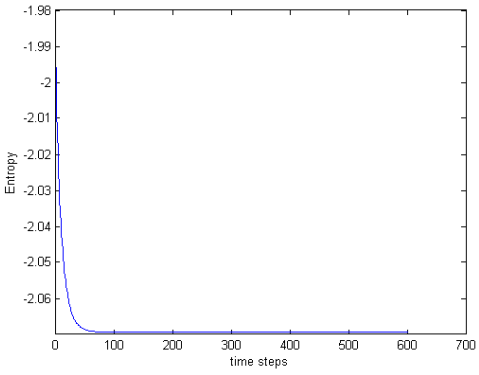

FIG. 15. *Test 3: The entropy decay of DG solutions for sudden heating problem.*

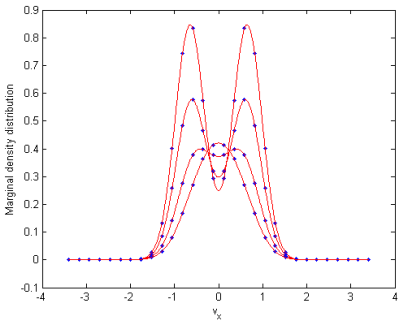

FIG. 16. *Test 4: Evolution of marginal distributions at* $t = 0, 1, 2.5, 5s$*; dots are the piecewise constant value on each element; solid lines are spline reconstructions.*

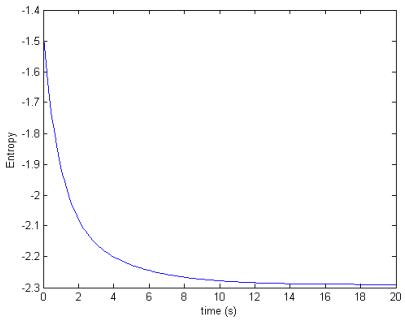

FIG. 17. *Test 4: Entropy decay.*

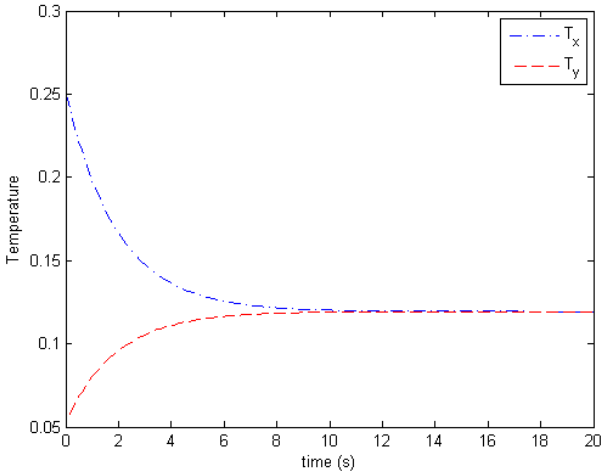

FIG. 18. *Test 4: Temperature relaxations along x and y directions.*

Test 4 is testing on the three-dimensional homogeneous Boltzmann equation with Maxwell molecular potential, with initial

$$f_0(\mathbf{v}) = \frac{1}{2(2\pi\delta^2)^{3/2}}\left[\exp\left(-\frac{|\mathbf{v}-2\delta\mathbf{e}|^2}{2\delta^2}\right)+\exp\left(-\frac{|\mathbf{v}+2\delta\mathbf{e}|^2}{2\delta^2}\right)\right],$$

where parameters $\delta = \pi/10$ and $\mathbf{e} = (1, 0, 0)$. $\Omega_{\mathbf{v}} = [-3.4, 3.4]^3$; $n = 30$.

Figure 16 shows the evolution of the marginal density distributions, which is defined as

$$f_x(\mathbf{v}_x \in I_k) = \frac{1}{(\Delta v)^3}\int_{I_k}\int_{I_{n/2}}\int_{I_{n/2}} f(\mathbf{v}, t)d\mathbf{v}_x d\mathbf{v}_y d\mathbf{v}_z.$$

Figure 17 shows the decay of entropy to its equilibrium state.

Figure 18 shows the relaxations of directional temperature, which as expected converge to the averaged temperature.

9. Summary and future work. In this paper, we introduced a conservative deterministic solver, based on DG methods, for the homogeneous Boltzmann equation. The tremendous computational cost of the collision matrix is successfully reduced by finding out a minimal basis set which can exactly reconstruct the complete family of matrix, and also by implementing parallel computing techniques, e.g., hybrid MPI and OpenMP. The temporal evolution is also parallelized. Our test computations have been distributed among up to 256 nodes and 4000 cores on clusters Lonestar and Stampede affiliated with TACC [47]. During the evaluations, we take the conservation laws into consideration and design a conservation routine to force the preservations of desired moments. The conservation routine also helps reduce the computational cost because it avoids the employment of higher order basis polynomials (actually piecewise constant basis functions are enough). The accuracy is guaranteed though asymptotic error analysis.

We believe this is a successful attempt on evaluating the full Boltzmann collisional operators under a DG method framework, which will be the base for future development of DG finite element methods for kinetic equations and applications to inhomogeneous transport equations for problems of nonsmooth density functions, irregular spatial domains, rough boundary conditions, etc.

Also, in the future, we will try to speed up the temporal evolution and test on more irregular problems with finer DG grids.

Appendix A. Tools for asymptotic behavior study of the DG conservative solver.

The classical Sobolev spaces are defined as

$$\begin{aligned} W^{\alpha,p}(\Omega) &= \{f \in L^p(\Omega) : D^\beta f \in L^p(\Omega) \quad \forall \text{ multi-indices } \beta \text{ such that } |\beta| \le \alpha\}, \\ H^\alpha(\Omega) &= W^{\alpha,2}(\Omega), \end{aligned} \tag{A.1}$$

and they are equipped with the norms

$$\begin{aligned} \|f\|_{W^{\alpha,p}(\Omega)} &= \sum_{|\beta|\le\alpha} \|D^\beta f\|_{L^p(\Omega)} \qquad \text{if } p < \infty, \\ \|f\|_{W^{\alpha,\infty}(\Omega)} &= \max_{|\beta|\le\alpha} \|D^\beta f\|_{L^\infty(\Omega)} \qquad \text{if } p = \infty. \end{aligned} \tag{A.2}$$

The *weighted Sobolev spaces* H^m_α are H^m spaces weighted with $\langle v\rangle^\alpha = \left(1 + |v|^2\right)^{\gamma\alpha/2}$. That is,

$$\|f\|_{H^m_\alpha(\Omega)} = \sum_{|\alpha|\le m} \|D^\alpha f \langle v\rangle^\alpha\|_{L^2(\Omega)}. \tag{A.3}$$

Here, please note that especially for the asymptotic error analysis for the DG solver, we include the intermolecular potential parameter γ here. The *broken Sobolev spaces* for the partition of Ω are defined as

$$\begin{aligned} W^{\alpha,p}(\mathcal{T}_h) &= \{f \in L^p(\Omega) : f|_E \in W^{\alpha,p}(E) \quad \forall\, E \in \mathcal{T}_h\}, \\ H^\alpha(\mathcal{T}_h) &= W^{\alpha,2}(\mathcal{T}_h), \end{aligned} \tag{A.4}$$

and the corresponding norms

$$\|f\|_{W^{\alpha,p}(\mathcal{T}_h)} = \sum_{E\in\mathcal{T}_h} \|f\|_{W^{\alpha,p}(E)} \qquad \text{if } p<\infty, \tag{A.5}$$

$$\|f\|_{W^{\alpha,\infty}(\mathcal{T}_h)} = \max_{E\in\mathcal{T}_h} \|f\|_{W^{\alpha,\infty}(E)} \qquad \text{if } p=\infty. \tag{A.6}$$

Then, we define the standard d-dimensional L^2 projection $P_h : f \mapsto P_h f$ by

$$\int_E P_h f(v)\phi(v)dv = \int_E f(v)\phi(v)dv \quad \forall \phi \in \mathbf{P}^l|_E. \tag{A.7}$$

By Poincare's inequality and Sobolev embedding theorems, we can prove the following approximation theory:

$$\begin{aligned}
&\|f - P_h f\|_{L^2(\mathcal{T}_h)} \lesssim h^{\alpha+1}\|f\|_{H^{\alpha+1}(\Omega)} \quad \forall f \in H^{\alpha+1}(\Omega),\\
&\|f - P_h f\|_{L^\infty(\mathcal{T}_h)} \lesssim h^{\alpha+1}\|f\|_{W^{\alpha+1,\infty}(\Omega)} \quad \forall f \in W^{\alpha+1,\infty}(\Omega),\\
&\|P_h f\|_{L^p(\mathcal{T}_h)} \lesssim \|f\|_{L^p(\Omega)} \quad \forall f \in L^p(\Omega), \quad 1\le p\le\infty,
\end{aligned}$$

where $h = \max_{E\in\mathcal{T}_h} \operatorname{diam}(E)$.

A.1. Extension operators. For fixed $\alpha_0 \ge 0$, there exists an extension operator $\mathrm{E} : L^2(\Omega_v) \to L^2(\mathbb{R}^d)$ such that for any $\alpha \le \alpha_0$ one has additionally $\mathrm{E} : H^\alpha(\Omega_v) \to H^\alpha(\mathbb{R}^d)$. The construction of such operator is well known and has following the properties [46]:

1. Linear and bounded with
$$\|\mathrm{E}f\|_{H^\alpha(\mathbb{R}^d)} \le C_\alpha \|f\|_{H^\alpha(\Omega_v)} \quad \text{for } \alpha \le \alpha_0.$$
2. $\mathrm{E}f = f$ a.e. in Ω_v.
3. Outside Ω_v the extension is constructed using a reflexion of f near the boundary $\partial\Omega_v$. Thus, for any $\delta \ge 1$ we can choose an extension with support in $\delta\Omega_v$, the dilation of Ω_v by δ, and
$$\|\mathrm{E}f\|_{L^p(\delta\Omega_v\setminus\Omega_v)} \le C_0\|f\|_{L^p(\Omega_v\setminus\delta^{-1}\Omega_v)} \quad \text{for } 1\le p\le 2,$$
where the constant C_0 is independent of the support of the extension.
4. In particular, properties 2 and 3 imply that for any $\delta \ge 1$ there is an extension such that
$$\|\mathrm{E}f\|_{L^p_k(\mathbb{R}^d)} \le 2C_0\delta^{2k}\|f\|_{L^p_k(\Omega_v)} \quad \text{for } 1\le p\le 2,\ k\ge 0.$$

A.2. Lemmas for asymptotic behavior study. Following the arguments in [3], we have the following.

LEMMA A.1 (elastic Lagrange estimate). *The problem* (5.2) *has a unique minimizer given by*

$$X^* = Q_u(f)(v) - \frac{1}{2}\Big(\gamma_1 + \sum_{j=1}^{d}\gamma_{j+1}v_j + \gamma_{d+2}|v|^2\Big),$$

where γ_j, for $1 \le j \le d+2$, are Lagrange multipliers associated with the elastic optimization problem. Furthermore, they are given by

$$\begin{aligned}\gamma_1 &= O_d\rho_u + O_{d+2}e_u\,,\\ \gamma_{j+1} &= O_{d+2}\mu_u^j\,, \quad j = 1, 2, \ldots, d,\\ \gamma_{d+2} &= O_{d+2}\rho_u + O_{d+4}e_u\,.\end{aligned}$$

The estimate constants $O_r := O(L^{-r})$ only depend inversely on $|\Omega_v|$. The parameters ρ_u, μ_u^j, e_u are density, momentum, and kinetic energy associated with the unconserved collision operator $Q_{uc}(f_h)$.

In particular, for dimension $d = 3$, the minimized objective function is given by

(A.8)
$$\mathcal{A}^e(X^*) = \|Q_u(f) - X^*\|^2_{L^2(\Omega_v)} = 2\gamma_1^2L^3 + \frac{2}{3}(\gamma_2^2+\gamma_3^2+\gamma_4^2)L^5 + 4\gamma_1\gamma_5L^5 + \frac{38}{15}\gamma_5^2L^7\,.$$

The minimizer is the expected conservation correction, i.e., $Q_c(f_h) = X^*$. So for the elastic case (conservation up to kinetic energy), the conserved projection operator $Q_c(f_h)$ is a perturbation of $Q_{uc}(f_h)$ by a second order polynomial.

In what follows we denote the moments of a function f by

$$m_k(f) := \int_{\mathbb{R}^d} \big|f(v)\big|\,|v|^{\gamma k}\,dv$$

and

$$Z_k(f) := \sum_{j=0}^{k-1} \begin{pmatrix} k \\ j \end{pmatrix} m_{j+1}m_{k-j}. \tag{A.9}$$

Besides the above lemma, we list several other results necessary for the final convergence and error estimate, most of which are generalized from the work [3].

LEMMA A.2 (conservation correction estimate). *Fix $f \in L^2(\Omega_v)$; then the accuracy of the conservation minimization problem is proportional to the spectral accuracy. That is, for any $k, k' \geq 0$ and $\delta > 1$, there exists some extension operator E such that*

$$\begin{aligned}\|\left(Q_c(f) - Q_u(f)\right)|v|^k\|_{L^2(\mathcal{T}_h)} \leq{}& \frac{C}{\sqrt{(k+d)}}L^{\gamma k}\|Q(Ef,Ef) - Q_u(f)\|_{L^2(\mathcal{T}_h)}\\ &+ \frac{\delta^{2\gamma k'}}{\sqrt{(k+d)}}O_{d/2+\gamma(k'-k)}\big(m_{k'+1}(f)m_0(f) + Z_{k'}(f)\big)\,,\end{aligned}$$

where C is a universal constant.

To prove our final convergence estimate, we need another theorem in the L^2-theory of the collision operator, which is the *Sobolev bound estimate*.

THEOREM A.3 (Sobolev bound estimate). *Let $\mu > \frac{d}{2} + \gamma$. For $f, g \in H^\alpha_{k+\mu}$, the collision operator satisfies*

$$\|Q(f,g)\|^2_{H^\alpha_k} \leq C\sum_{j\leq\alpha}\binom{\alpha}{j}\left(\|f\|^2_{H^{\alpha-j}_{k+\gamma}}\|g\|^2_{H^j_{k+\mu}} + \|f\|^2_{H^{\alpha-j}_{k+\mu}}\|g\|^2_{H^j_{k+\gamma}}\right), \tag{A.10}$$

where the dependence of the constant is $C := C(d, \beta, \alpha, \|b\|_1)$.

And also, we need the following H^α_k-norm propagation properties of the solutions.

LEMMA A.4 (H^α_k-norm propagation). *Assume $f_{h,0} \in H^\alpha_{k+1+\alpha}(\Omega_v)$; then there exists an extension operator E_α such that, for any time T, we can choose a lateral*

size $L_0(f_0, k, \alpha)$ for the truncated domain Ω_v such that for any $L \geq L_0$ there exists a small mesh size $h_0 = \max_{E_v \in \mathcal{T}_h} diam(E_v)$,

$$\sup_{t\in[0,T]} \|f_h\|_{H^\alpha_k(\Omega_v)} \leq \max\left\{\|f_{h,0}\|_{H^\alpha_{k+1+\lambda}(\Omega_v)}, C_k(m_{k'}(g_0))\right\}, \quad h \leq h_0,$$

where $k' \geq k$ is a finite number of moments. Additionally, C_k is independent of the parameters L.

Acknowledgment. Support from the Institute of Computational Engineering and Sciences (ICES) at the University of Texas Austin is gratefully acknowledged.

REFERENCES

[1] A. Alekseenko and E. Josyula, *Deterministic solution of the Boltzmann equation using discontinuous Galerkin discretizations in velocity space*, J. Comput. Phys., 272 (2014), pp. 170–188.

[2] R. Alonso, J. Canizo, I. Gamba, and C. Mouhot, *A new approach to the creation and propagation of exponential moments in the Boltzmann equation*, Comm. Partial Differential Equations, 38 (2013), pp. 155–169.

[3] R. Alonso, I. M. Gamba, and S. H. Tharkabhushaman, *Convergence and Error Estimates for the Lagrangian Based Conservative Spectral Method for Boltzmann Equations*, preprint, arXiv:1611.04171v2 [math.NA], 2017.

[4] V. V. Aristov, *Direct Methods for Solving the Boltzmann Equation and Study of Nonequilibrium Flows*, Fluid Mech. Appl. 60, Springer, New York, 2001.

[5] G. A. Bird, *Molecular Gas Dynamics*, Clarendon Press, Oxford, UK, 1994.

[6] A. V. Bobylev, *Exact solutions of the nonlinear Boltzmann equation and the theory of relaxation of a Maxwellian gas*, Teoret. Mat. Fiz, 60 (1984), pp. 280–310.

[7] A. V. Bobylev and C. Cercignani, *Discrete velocity models without nonphysical invariants*, J. Stat. Phys., 97 (1999), pp. 677–686.

[8] A. V. Bobylev, I. M. Gamba, and V. A. Panferov, *Moment inequalities and high-energy tails for Boltzmann equations with inelastic interactions*, J. Stat. Phys., 116 (2004), pp. 1651–1682.

[9] A. V. Bobylev and S. Rjasanow, *Difference scheme for the Boltzmann equation based on the fast Fourier transform*, Eur. J. Mech. B Fluids, 16 (1997), pp. 293–306.

[10] A. V. Bobylev and S. Rjasanow, *Numerical solution of the Boltzmann equation using fully conservative difference scheme based on the fast Fourier transform transport theory*, J. Stat. Phys., 29 (2000), pp. 289–310.

[11] A. V. Bobylev and S. Rjasanow, *Fast deterministic method of solving the Boltzmann equation for hard spheres*, Eur. J. Mech. B Fluids, 18 (1999), pp. 869–887.

[12] J. E. Broadwell, *Study of rarefied shear flow by the discrete velocity method*, J. Fluid Mech., 19 (1964), pp. 401–414.

[13] H. Cabannes, *Global solution of the initial value problem for the discrete Boltzmann equation*, Arch. Mech. (Arch. Mech. Stos.), 30 (1978), pp. 359–366.

[14] C. Cercignani, *The Boltzmann Equation and Its Applications*, Springer-Verlag, New York, 1988.

[15] C. Cercignani and H. Cornille, *Shock waves for a discrete velocity gas mixture*, J. Stat. Phys., 99 (2000), pp. 115–140.

[16] Y. Cheng, I. M. Gamba, A. Majorana, and C.-W. Shu, *A discontinuous Galerkin solver for Boltzmann Poisson systems in nano devices*, Comput. Methods Appl. Mech. Engr., 198 (2009), pp. 3130–3150.

[17] Y. Cheng, I. M. Gamba, A. Majorana, and C.-W. Shu, *A brief survey of the discontinuous Galerkin method for the Boltzmann-Poisson equations*, SeMA J., 54 (2011), pp. 47–64.

[18] Y. Cheng, I. M. Gamba, A. Majorana, and C.-W. Shu, *Discontinuous Galerkin methods for the Boltzmann-Poisson systems in semiconductor device simulations*, AIP Conference Proceedings, 1333 (2011), pp. 890–895.

[19] Y. Cheng, I. M. Gamba, A. Majorana, and C.-W. Shu, *A discontinuous Galerkin solver for full-band Boltzmann-Poisson models*, in Proceedings of the 13th International Workshop on Computational Electronics, 2009, pp. 211–214.

[20] Y. Cheng, I. M. Gamba, and J. Proft, *Positivity-preserving discontinuous Galerkin schemes for linear Vlasov-Boltzmann transport equations*, Math. Comp., 81 (2012), pp. 153–190.

[21] B. Cockburn and C.-W. Shu, *Runge-Kutta discontinuous Galerkin methods for convection-dominated problems*, J. Sci. Comput., 16 (2001), pp. 173–261.
[22] M. H. Ernst, *Exact solutions of the nonlinear Boltzmann equation and related kinetic models*, in Nonequilibrium Phenomena I, Stud. Statist. Mech. 10, North-Holland, Amsterdam, 1983, pp. 51–119.
[23] F. Filbet, C. Mouhot, and L. Pareschi, *Solving the Boltzmann equation in NLOGN*, SIAM J. Sci. Comput., 28 (2006), pp. 1029–1053.
[24] F. Filbet and G. Russo, *High order numerical methods for the space non homogeneous Boltzmann equation*, J. Comput. Phys., 186 (2003), pp. 457–480.
[25] E. Gabetta, L. Pareschi, and G. Toscani, *Relaxation schemes for nonlinear kinetic equations*, SIAM J. Numer. Anal., 34 (1997), pp. 2168–2194.
[26] E. Gabriel, G. E. Fagg, G. Bosilica, T. Angskun, J. J. Dongarra, J. M. Squyres, V. Sahay, P. Kambadur, B. Barrett, A. Lumsdaine, R. H. Castain, D. J. Daniel, R. L. Graham, and T. S. Woodall, *Open MPI: Goals, concept, and design of a next generation MPI implementation*, in Proceedings of the 11th European PVM/MPI Users' Group Meeting, 2004, pp. 97–104.
[27] M. Galassi, J. Davies, J. Theiler, B. Gough, G. Jungman, P. Alken, M. Booth, and F. Rossi, GNU Scientific Library Reference Manual, 3rd ed., Network Theory, UK, 2009, http://www.gnu.org/software/gsl/.
[28] I. M. Gamba, V. Panferov, and C. Villani, *Upper Maxwellian bounds for the spatially homogeneous Boltzmann equation*, Arch. Rat. Mech. Anal, 194 (2009), pp. 253–282.
[29] I. M. Gamba and S. H. Tharkabhushaman, *Spectral-Lagrangian based methods applied to computation of non-equilibrium statistical states*, J. Comput. Phys., 228 (2009), pp. 2012–2036.
[30] I. M. Gamba and S. H. Tharkabhushaman, *Shock and boundary structure formation by spectral-Lagrangian methods for the inhomogeneous Boltzmann transport equation*, J. Comput. Math, 28 (2010), pp. 430–460.
[31] J. R. Haack and I. M. Gamba, *conservative spectral method for the Boltzmann equation with anisotropic scattering and the grazing collisions limit*, J. Comput. Phys., 270 (2014), 40.
[32] J. R. Haack and I. M. Gamba, *High performance computing with a conservative spectral Boltzmann solver*, AIP Conference Proceedings 1501, 334 (2012).
[33] M. Herty, L. Pareschi, and M. Seaid, *Discrete-velocity models and relaxation schemes for traffic flows*, SIAM J. Sci. Comput., 28 (2006), pp. 1582–1596.
[34] W. Hoitinga and E.H. van Brummelen, *A discontinuous Galerkin finite-element method for a 1D prototype of the Boltzmann equation*, J. Comput. Phys., 230 (2011), pp. 6115–6135.
[35] I. Ibragimov and S. Rjasanow, *Numerical solution of the Boltzmann equation on the uniform grid*, Computing, 69 (2002), pp. 163–186.
[36] R. Illner, *On the derivation of the time-dependent equations of motion for an ideal gas with discrete velocity distribution*, J. de Mecanique, 17 (1978), pp. 781–796.
[37] S. Kawashima, *Global solution of the initial value problem for a discrete velocity model of the Boltzmann equation*, Proc. Japan Acad. Ser. A Math. Sci., 57 (1981), pp. 19–24.
[38] A. Majorana, *A numerical model of the Boltzmann equation related to the discontinuous Galerkin method*, Kinet. Relat. Models, 4 (2011), pp. 139–151.
[39] L. Mieussens, *Discrete-velocity models and numerical schemes for the Boltzmann-BGK equation in plane and axisymmetric geometries*, J. Comput. Phys., 162 (2000), pp. 429–466.
[40] K. Nanbu, *Direct simulation scheme derived from the Boltzmann equation in monocomponent gases*, J. Phys. Soc. Japan, 52 (1983), pp. 2042–2049.
[41] OpenMP Architecture Review Board, *OpenMP Application Program Interface Version* 3.0, 2008, http://www.openmp.org/mp-documents/spec30.pdf.
[42] L. Pareschi and B. Perthame, *A Fourier spectral method for homogenous Boltzmann equations transport theory*, J. Stat. Phys., 25 (2002), pp. 369–382.
[43] L. Pareschi and G. Russo, *Numerical solution of the Boltzmann equation.* I. *Spectrally accurate approximation of the collision operator*, SIAM J. Numer. Anal. 37 (2000), pp. 1217–1245.
[44] S. Rjasanow and W. Wagner, *A stochastic weighted particle method for the Boltzmann equation*, J. Comput. Phys., 1996, pp. 243–253.
[45] S. Rjasanow and W. Wagner, *Stochastic Numerics for the Boltzmann Equation*, Springer, Berlin, 2005.
[46] E. Stein, *Singular Integrals and Differentiability Properties of Functions*, Princeton University Press, Princeton, NJ, 1970.
[47] Texas Advanced Computing Center (TACC), The University of Texas at Austin, http://www.tacc.utexas.edu.

[48] A. B. Morris, P. L. Varghese, and D. B. Goldstein, *Variance Reduction for a Discrete Velocity Gas*, 27th International Symposium on Rarefied Gas Dynamics 2010, AIP Conf. Proc. 1333 (2011), pp. 952–957.

[49] A. B. Morris, P. L. Varghese, and D. B. Goldstein, *Monte Carlo solution of the Boltzmann equation via a discrete velocity model*, J. Comput. Phys., 230 (2011), pp. 1265–1280.

[50] A. B. Morris, P. L. Varghese, and D. B. Goldstein, *Improvement of a discrete velocity Boltzmann equation solver with arbitrary post-collision velocities*, Rarefied Gas Dynamics, 26th International Symposium on Rarefied Gas Dynamics, ed. T. Abe, Kyoto, AIP Conf. Proc. 1084 (2009), pp. 458–463.

[51] C. Zhang and I. M. Gamba, *A conservative discontinuous Galerkin scheme with $O(N^2)$ operations in computing the Boltzmann collision weight matrix*, Rarefied Gas Dynamics, 29th International Symposium on Rarefied Gas Dynamics, AIP Conf. Proc. 1628 (2014), pp. 75–83.

[52] C. Zhang and I. M. Gamba, *A conservative scheme for Vlasov Poisson Landau modeling collisional plasmas*, J. Comput. Phys., 340 (2017), pp. 470–497.

[53] C. Zhang and I. M. Gamba, *Spectral Gap Computations for Linearized Boltzmann Operators*, preprint, arXiv:1807.09868v1 [math-ph], 2018, https://arxiv.org/abs/1807.09868v1.

[54] X. Zhang and C.-W. Shu, *On positivity preserving high order discontinuous Galerkin schemes for compressible Euler equations on rectangular meshes*, J. Comput. Phys., 229 (2010), pp. 8918–8934.

[55] Y. Zheng and H. Struchtrup, *A linearization of Mieussens's discrete velocity model for kinetic equations*, Eur. J. Mech. B Fluids, 26 (2007), pp. 182–192.